16 State House Station
Augusta, Maine 04333

MaineDOT

Transportation Research Division

Technical Report 16-15

Advanced Bridge Safety Initiative: Phase 2

Task 3- *Instrumentation During Live Load Testing and Load Rating of Five Reinforced Concrete Slab Bridges*

May 2016

Technical Report Documentation Page

1. Report No. ME 16-15	2.	3. Recipient's Accession No.	
4. Title and Subtitle Advanced Bridge Safety Initiative: Phase 2, Task 3 - Instrumentation During Live Load Testing and Load Rating of Five Reinforced Concrete Slab Bridges		5. Report Date May 2016 6.	
7. Author(s) Scott Tomlinson P.E., William Davids Ph.D, P.E.		8. Performing Organization Report No. 16-23-1332.3	
9. Performing Organization Name and Address Advanced Structures and Composites Center University Of Maine 35 Flagstaff Rd. Orono, ME 04469		10. Project/Task/Work Unit No. Project 017666.00 11. Contract © or Grant (G) No. Contract # 20160617*4564	
12. Sponsoring Organization Name and Address Maine Department of Transportation		13. Type of Report and Period Covered 14. Sponsoring Agency Code	
15. Supplementary Notes			

16. Abstract (Limit 200 words)

Five reinforced concrete slab bridges were tested during the summer of 2015 by the University of Maine (UMaine) as part of this program: 1. Weld No. 5361, 2. West Paris No. 2582, 3. Wiscasset/ Woolwich No. 2577, 4. Penobscot No. 3297, and 5. Smyrna No. 2250. Revised load ratings were computed using either test data or with more detailed analyses than provided to UMaine by the Maine Department of Transporation (MaineDOT). Testing instrumentation setups, loading setups, and strain plots for each bridge are provided in Appendices A.1, A.2, A.3, A.4, and A.5. The results of the tests and analyses are summarized and compared with the existing ratings. Use of the these revised load ratings, live load test data, and extrapolation of these results to other structures is at the sole discretion of the bridge owner.

17. Document Analysis/Descriptors Bridge load rating, concrete slab, live load tests		18. Availability Statement	
19. Security Class (this report)	20. Security Class (this page)	21. No. of Pages 44	22. Price

Instrumentation During Live Load Testing and Load Rating of Five Reinforced Concrete Slab Bridges

Prepared for:
Dale Peabody P.E.
Director Transportation Research
Maine Dept. of Transportation
16 State House Station
Augusta ME 04333-0016
University of Maine's Advanced Structures and Composites Center
Report Number: 16-23-1332.3

2016-05-03-Rev00

Prepared by:
William Davids Ph.D. PE
John C. Bridge Professor of Civil and Environmental Engineering

Scott Tomlinson PE SCWI
Research Engineer

Reviewed by:
Joshua Clapp PE
Research Engineer

The University of Maine Advanced Structures and Composites Center is an ISO 17025 accredited testing laboratory, accredited by the International Accreditation Service.

Advanced Structures and Composites Center
35 Flagstaff Rd
University of Maine
Orono, ME 04469

Telephone: 207-581-2123
FAX: 207-581-2074
composites@maine.edu
www.composites.umaine.edu

Document Log

Name/ Organization	Date	Version	Action
William Davids, Author Scott Tomlinson, Author Joshua Clapp, Reviewer	2016-05-03	Rev00	Initial release to MaineDOT.

Table of Contents

Index of Figures

Index of Tables

Acronyms

AASHTO MBE: American Association of State Highway and Transportation Officials Manual for Bridge Evaluation
AASHTO: American Association of State Highway and Transportation Officials
BDI: Bridge Diagnostics Inc.
LRFD: Load Resistance Factor Design
Maine DOT: Maine Department of Transportation

STS-WiFi: Wireless Structural Testing System
UBIT: Under Bridge Inspection Truck
UMaine: The University of Maine

Executive Summary

Five reinforced concrete slab bridges were tested during the summer of 2015 by the University of Maine (UMaine) as part of this program: 1. Weld No. 5361, 2. West Paris No. 2582, 3. Wiscasset/ Woolwich No. 2577, 4. Penobscot No. 3297, and 5. Smyrna No. 2250. Revised load ratings were computed using either test data or with more detailed analyses than provided to UMaine by the Maine Department of Transporation (MaineDOT). Testing instrumentation setups, loading setups, and strain plots for each bridge are provided in Appendices A.1, A.2, A.3, A.4, and A.5. The results of the tests and analyses are summarized below and compared with the existing ratings. Use of the these revised load ratings, live load test data, and extrapolation of these results to other structures is at the sole discretion of the bridge owner.

1. Weld No. 5361: Although the clear span of this bridge was longer than the others tested, measured strains on this bridge were among the lowest. Based on revised analysis of the bridge for one truck at a time, positive moment at midspan, for HL-93 the inventory rating was found to be 1.47 when using the *SlabRate* finite-element program.
2. West Paris No. 2582: Based on existing geometry with the original and widened slabs each supporting a lane with very little interaction, MaineDOT may choose to focus on single lane rating factors. Analyzing the widened slab with one lane loaded and based on strains measured in testing, the rating factors were found to increase from 0.75 to 1.17 for HL-93 inventory loading and from 0.97 to 1.51 for HL-93 operating loading.
3. Wiscasset/ Woolwich No. 2577: Low loads compared to HL-93 + impact were applied by the crane used to load the structure. MaineDOT may choose to upgrade the rating factor despite these low loads based on assumptions discussed futher in Section 2.3.
4. Penobscot No. 3297: The geometry of this bridge, with an original slab in the center and widened portions on both sides holding sidewalks with curbs and guardrails, required several sets of assumptions to be considered in the revised rating factors. These sets of assumptions, including boundary conditions between the old and new slabs, concrete wearing surface thickness, and reinforcing are further discussed in Section 2.4.2.
5. Smyrna No. 2250: The new widened portion of the road was analyzed, and the predicted strains were significantly greater than measured strains, with a minimum ratio of predicted/ measured of 2.02. However, due to the low loads compared to HL-93 + impact, no rating factor recommendation is made.

1 Bridge Testing Program

Five slab type reinforced concrete bridges were tested during the summer of 2015 as part of this program: 1. Weld No. 5361, 2. West Paris No. 2582, 3. Wiscasset/ Woolwich No. 2577, 4. Penobscot No. 3297, and 5. Smyrna No. 2250. Bridges were instrumented with a strain measuring system, loaded with heavy vehicular loads, and then analyzed to determine whether it may be reasonable to change the bridge rating factors based on the testing and refined analysis.

1.1 Instrumentation

The strain measurement system utilized in this research is a partially Wireless Structural Testing System (STS-WiFi) by Bridge Diagnostics Inc. (BDI). The system used for this testing utilized a mobile base station to communicate with up to 6 nodes with up to 4 strain sensors per node and an additional autoclicker node for monitoring tire rotation of loading vehical. This system communicated with a dedicated laptop running BDI specific WinSTS data acquisition software. This system was fully verified in the laboratory prior to use in the field. This verification consisted of first mounting the gages to steel spacers utilized in calibrated tension testing servo-hydraulic Instron actuators and verifying that measured strains were as predicted. Next, the system was utilized to instrument a 35 ft. long concrete beam undergoing bending testing. Strains were predicted utilizing both mechanics based calculations and advanced three-dimensional finite element analysis, and matched measured strains well. A sample setup in the field is shown in Figure 1, with strain sensors mounted under the bridge at mid-span connected to battery operated wireless nodes connected to the guardrail. A clear diagram of the entire network is shown in Figure 2 including strain sensors, wireless nodes, the wirelss base station, autoclicker, and the data recording laptop.

Figure 1: Typical strain sensors mounted under bridge connected to wireless nodes

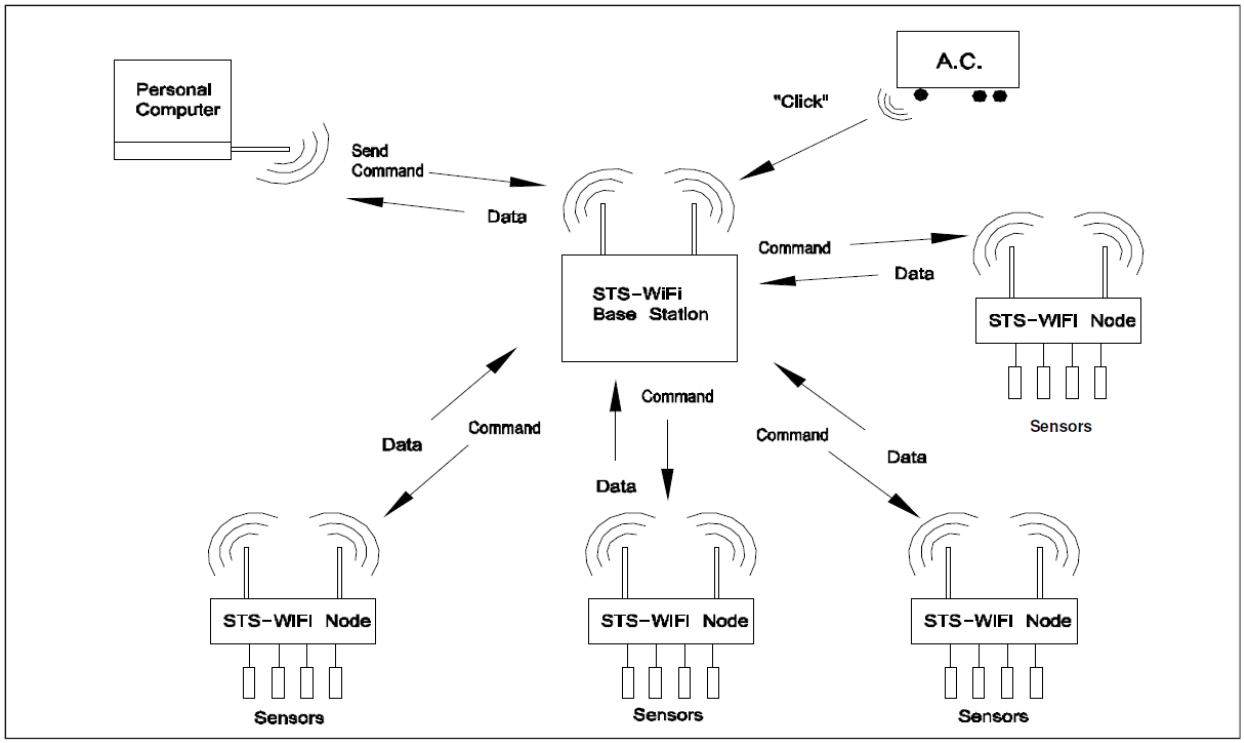

Figure 2: BDI STS-Wifi network setup for bridge sensor setup.

Strain sensors were mounted under the bridges using a MaineDOT Under Bridge Inspection Truck (UBIT) as shown in Figure 3. The sensors were mounted to the concrete by first grinding the concrete to a fresh surface, cleaning the surface, then using the recommended concrete adhesive to connect the strain sensor tabs to the concrete. Strain sensor layout was optimized for each bridge, with individual sensor layouts shown in the appendicies.

Figure 3: MaineDOT UBIT utilized to install sensors

1.2 Loading

The crane used for this testing was a Grove TMS900E as shown in Figure 4. The crane was weighed using state patrol certified portable scales as shown in Figure 5. Each test was run with crane moving both directions on each side of the road in optimized load paths as is detailed in the appendicies. In general, this was as close to the curb on both sides as possible to maximize the moment along the free edge of the bridge. The autoclicker was utilized to create marks in the data acquisition system at each wheel rotation to determine the vehicle location during the test, and the setup is shown in Figure 6.

Figure 4: Grove TMS 900E crane used for bridge loading

Figure 5: State highway patrol certified portable crane scales used to verify vehicle weight for each test

Figure 6: Autoclicker setup to measure wheel rotations for data analysis

1.3 Analysis

Analysis of the bridges tested is described in detail in Section 2. In general, hand calculations based on mechanics of materials principles, American Association of State Highway and Transportation Officials (AASHTO) code requirements including the Manual for Bridge Evaluation (AASHTO MBE) were first conducted. Finite element modeling is conducted where required utilizing *SlabRate* software, a custom program written in MATLAB by the project PI.

2 Analysis of Live Load Test Data

2.1 Weld No. 5361

The highest measured strain recorded from the live load test of Weld No. 5361 was 34 με, which is low relative to the other four bridges tested. While the bridge has the longest clear span of all tested slabs at 360 in, the 19 in thick structural slab was likely stiffened by the additional 3 in concrete wearing surface noted on the plans. A review of the load rating analysis performed by the MaineDOT using input values from a load rating conducted independently by a consultant showed the main reinforcing steel as 1.25 in diameter bars spaced at 7.75 in on center, giving a steel area of 1.9 in^2/ft. The MaineDOT load rating conducted per *SlabRate* yielded an HL-93 inventory rating of 0.91. However, the plans indicate #11, 1.25 in square bars with a cross-sectional area of 1.56 in^2 each. Further, the bar spacing of 7.75 shown on the plans is along the 30 degree skew, and the actual bar spacing parallel to the span is 6.71 in. Therefore, the actual

steel area is 2.79 in^2/ft. This increases the HL-93 inventory rating to 1.47 when using the *SlabRate* finite-element program. No further analyses were completed given that Weld No. 5361 appears to be in excellent condition, as shown in Figure 7 and has an inventory rating factor substantially greater than one.

Figure 7: Weld No. 5361 general condition

2.2 West Paris No. 2582

2.2.1 Finite-Element Analysis of West Paris No. 2582 and Comparison with Field Data

The highest measured strains were recorded during Test 08 in the widened portion of the structure. This is consistent with the thinner slab (16.5 in) in the widened portion compared with the original 20 in slab. The two slabs are separated by a cold joint containing a bond breaker as shown in Figure 8, and therefore should behave largely independently. This was confirmed by the very small measured strains in the original portion of the structure when the widened portion was loaded. The finite-element analysis of the slab was thus performed for the critical, widened portion of the structure only. The slab width tapers from 18 ft 7 in to 20 ft 7 in with a 1 ft curb. An average overall width of 19 ft 7 in was assumed for all analyses, and the effect of the thickened curbs was not modeled. A full-depth, un-cracked section was assumed for all analyses, which is consistent with the small measured longitudinal strains of less than 40 με. The model had 20 elements in both the longitudinal and transverse directions, and strains were interpolated at the gauge locations using nodal values output by the model.

Figure 8: West Paris No. 2582 joint and general condition

The AASHTO MBE recommends that the concrete strength be taken as 2.5 ksi based on the 1951 construction date. However, it is likely that the actual strength is significantly greater than the nominal value of 2.5 ksi. Further, a lower-than-actual concrete strength will lead to higher model-predicted strains, which is unconservative when computing a rating factor modifier per the AASHTO MBE. Therefore, the concrete compressive strength was assumed to be 4 ksi with a corresponding elastic modulus of 3600 ksi.

Strains were computed assuming isotropic, thin plate theory, which accounts for the effect of both longitudinal and transverse bending moments. Figure 9 shows the model-predicted strains as a function of truck position at the locations of the gauges installed on the bottom of the slab at mid-span.

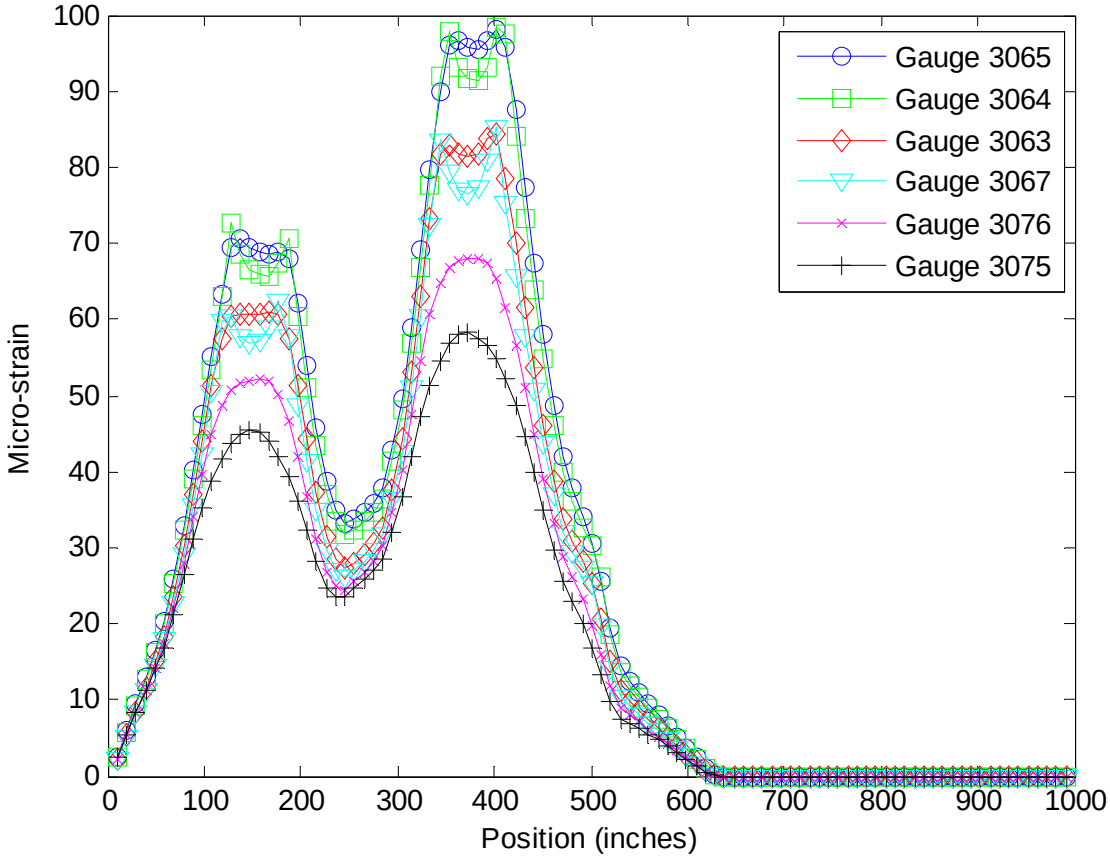

Figure 9: Finite-element predicted strains for West Paris No. 2582

The relative magnitudes of the predicted strains are in good qualitative agreement with measured strains. One discrepancy is that the largest measured strains occurred at gauge 3063, whereas the model predicts the largest measured strains at gauge locations 3064 and 3065. This could be due to the integral concrete curb that is nearest to gauges 3064 and 3065, the effect of which is not captured by the finite-element model. To quantify the discrepancy between the FE model-predicted strain ε_c and measured strain ε_T, peak values for each and the ratio $\varepsilon_T/\varepsilon_c$ are presented in Table 1 for each gauge location.

Table 1: Peak measured and model-predicted strains for West Paris No. 2582

Gauge Location	Measured Peak ε_T (με)	Predicted Peak ε_c (με)	$\varepsilon_c/\varepsilon_T$
3065	38.3	98.0	2.56
3064	35.7	98.3	2.75
3063	39.6	84.3	2.13
3067	35.0	85.1	2.43
3076	20.9	68.1	3.26
3075	17.3	58.2	3.36

2.2.2 Modification of Single-Lane Rating Factor for West Paris Bridge No. 2582

An independent HL-93 operating load rating was completed by the MaineDOT for the widened portion of the West Paris bridge using the finite-element software *SlabRate*. According to the AASHTO MBE, a bridge with a roadway width of between 18 ft and 20 ft must be rated for two lanes of loading. The roadway width for the widened version of the West Paris slab varies from 17 ft 7 in to 19 ft 7 in, giving an average of 18 ft 7 in. However, the entire bridge has a roadway width of 40 ft, and is striped for only two lanes with 8 ft shoulders. Therefore, under current traffic conditions, one lane is entirely on the widened portion of the structure. Further, the interior edge of the slab near the lane edge is thickened, and the exterior slab edge has an integral curb. This implies that critical rating factors computed per the rating analysis at the slab edges will be conservative. Given these geometric considerations and the current striped lanes on the bridge, the MaineDOT may want to focus only on the rating corresponding to a single lane of loading, for which the HL-93 inventory and operating rating factors are 0.75 and 0.97, respectively.

A quick calculation of the maximum simple-span, single-lane bending moment produced by the crane used to test the West Paris structure gives a moment of 257 ft-kips per lane of loading (the calculation conservatively ignored the small contribution from the rear trailer axle). The moment due to an HL-93 tandem with impact plus lane load is 300 ft-kips for the same 20 ft 1 in span. Thus, the crane used to load the structure applied 257/(1.2*300) = 0.71 of an HL-93 service load with impact, after accounting for the single-lane multiple presence factor of 1.2. Assuming results cannot be extrapolated to higher loads, this corresponds to a K_b of 0.5 per Table 8.8.2.3.1-1 of the AASHTO MBE. The value of K_a is computed per AASHTO as $\varepsilon_c / \varepsilon_T - 1$, which is 1.13 based on the most conservative ratio of computed to measured strain given in Table 1. The rating factor adjustment $K = 1 + K_a K_b = 1 + 0.5*1.13 = 1.56$, implying that the HL-93 inventory and operating rating factors for a single lane of loading can be increased to 1.17 and 1.51, respectively.

2.3 Finite-Element Analysis of Wiscasset/ Woolwich No. 2577 and Comparison with Field Data

For load tests of bridge No. 2577, the crane produced only 62% of a single lane of HL-93 live loading with impact. As discussed previously, the measured strains were quite low (less than 20 με maximum positive strain for all loadings). This is likely due to several factors. First, the bridge has approximately 20 inches of fill over the top of the slab, which will tend to spread the wheel loads significantly. Secondly, the crane was not placed as close to the slab edge as in other tests. Third, the crane's heavy axles were relatively light for this test compared to the test at Weld and West Paris. Finally, the exterior edge of the slab, to which the crane was placed closest for the slow speed passes, has a significant integral curb. The general condition is shown in Figure 10. The effectiveness of this integral curb in carrying moments at the slab edge is

reflected in the large negative strains that developed in the gauge mounted on the top of the curb, especially in the newer (widened) portion of the slab as shown in Figure 11.

Figure 10: Woolwich No. 2577 showing integral curb and fill thickness

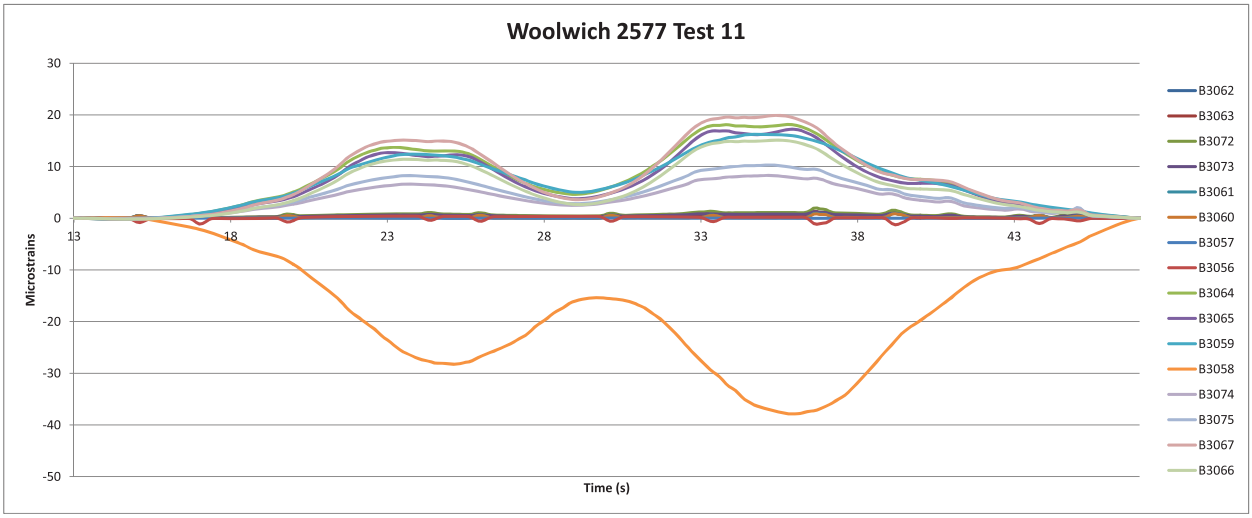

Figure 11: Woolwich No. 2577, test 11

A finite-element analysis of the newer portion of the structure was conducted for comparison with the field data gathered during test 11. The newer portion was chosen for comparison because it is narrower than the original structure, and therefore strains were more uniform across the width of the slab. The model had 20 elements in both the longitudinal and transverse directions, and strains were interpolated at the gauge locations using nodal values output by the

model. Given the small measured strains, the gross un-cracked section was used for all calculations.

Figure 12 shows predicted strains at the bottom of the slab. The model shows the largest strains at gages 3064, 3065, 3066 and 3067, which is generally consistent with the field data. The truck was positioned such that a wheel line traveled over gauges 3066 and 3067. One discrepancy is that the model predicts the largest strain at the location of gauge 3064, whereas peak strain was measured during the test at gauge 3067. However, comparison of the measured and predicted strains indicates that the FE model is consistently over-predicting the measured strains, which were a maximum of 20 με. This indicates there is potentially a significant degree of conservatism in the finite-element model.

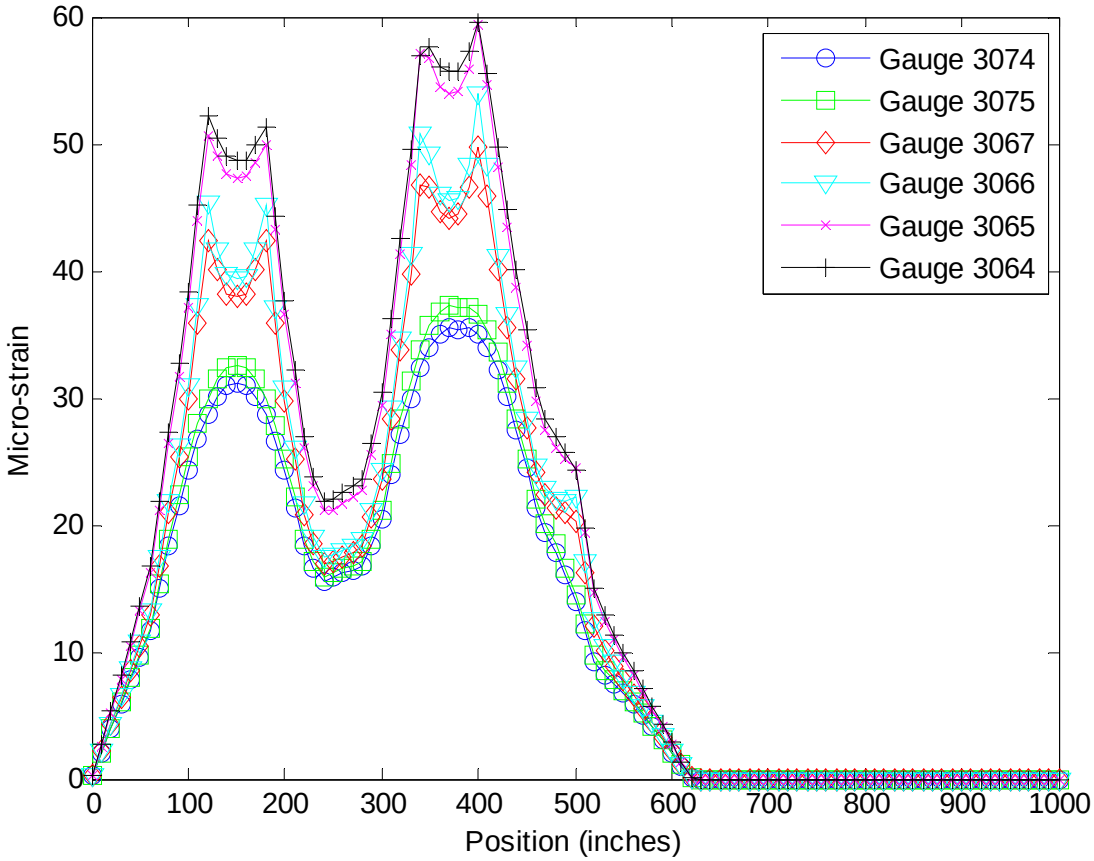

Figure 12: Finite-element predicted strains for Wiscasset/ Woolwich No. 2577

Despite the relatively small measured strains, the AASHTO MBE does not allow rating factors to be increased directly based on measured strains as could be done with bridge No. 2582 because of the relatively low load level and the uncertainty associated with extrapolating strains to larger loads. However, the low measured strains and service conditions may allow a revised

load rating to be conducted at the discretion of the MaineDOT. To explore this further, UMaine performed a load rating on the older, more critical structure with the following assumptions:

1. The original structure is assumed to carry only a single lane of loading. This is based on the existing lane striping, which will prevent a second lane of traffic from significantly loading the original structure under normal usage. The strain data gathered with the crane driving in traffic substantiates this: when the truck traveled down each lane with traffic, hugging the bridge centerline, the adjacent structure experienced small strains.
2. The tire contact width can be increased 20 inches, or the fill depth, in both the longitudinal and transverse directions. The increase in contact area parallel to the traffic direction is explicitly permitted by Chapter 4 of the AASHTO Load and Resistance Factor Design (LRFD) Specification for buried box culverts having less than 2 feet of fill. It is assumed that the same increase applies perpendicular to the traffic direction. Thus, the AASHTO standard 10 inch long by 20 inch wide tire patch will be increased to 30 inches long by 40 inches wide.
3. The critical location for load rating will be assumed near the slab edge closest to the bridge centerline. The plans show that the 18 inch wide integral curb was left protruding approximately 12 inches above the top of the slab during widening. This existing curb section will substantially strengthen and stiffen the structure at this location; however, this thickened curb has not been taken into account in the initial revised load rating.

Using these assumptions, the *SlabRate* analysis predicts an HL-93 operating rating of 0.92[1]. For comparison, an otherwise identical single-lane rating analysis assuming a conventional wheel load patch of 10 inches by 20 inches that was positioned entirely on the slab at its interior edge yielded an HL-93 operating rating factor of 0.75[2].

The critical location for the rating factor is, as expected, at the interior slab edge. However, this edge has a buried integral curb, which will increase capacity at this location. To explore this, an additional rating was conducted using the above assumptions, but the *SlabRate* FE model was modified to incorporate 32 inch thick, 18 inch wide elements at each slab edge to capture the effect of the thickened curb. The thickened curb sections are significantly stiffer than the slab alone, and tend to increase moments substantially at the slab edge. This is illustrated in Figure 13 with scaled color maps of HL-93 tandem with impact plus lane load moments in the constant thickness slab and the slab with thickened edge elements that account for the curb.

[1] Wisscasset/ Woolwich No. 2577: Assumption set 1
[2] Wisscasset/ Woolwich No. 2577: Assumption set 2

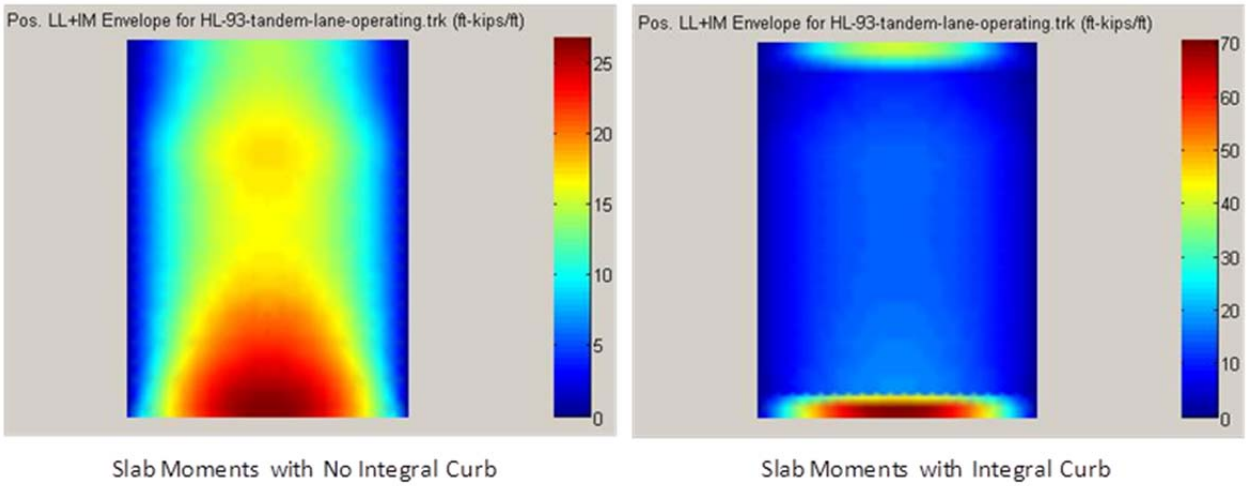

Figure 13: Effect of integral curb on predicted slab moments

The largest moments will in general be carried by the section of slab plus curb. A hand calculation was performed assuming the combined slab and curb to be an 18 inch wide by 32 inch deep beam reinforced with 3-#9 bars per the original plans. Using the capacity of this deeper section and the DC, DW and LL moments predicted at the outer slab edge, the operating rating factor at the curb increase to 1.01 for the HL-93 tandem[3].

To assess the capacity of the 20 inch thick portion of the slab near the thickened edge, the rating factor at a distance 6" in from the curb was computed to be 1.82 for the HL-93 tandem (operating)[4].

These results indicate that the bridge may have a sufficient rating capacity provided the MaineDOT is willing to accept the very specific and potentially un-conservative assumptions used in the single-lane rating analysis. Further, simply thickening the slab elements to account for the integral curb is a 2D simplification of the actual 3D bridge geometry, and the accuracy of this approach has not been verified.

2.4 Penobscot No. 3297

2.4.1 FE Analysis of Penobscot No. 3297 and Comparison with Field Data

The Penobscot bridge consists of an original section constructed in the 1930s and widened portions at both edges. The original portion of the structure carries most of both striped lanes, and the newer sections on each side are primarily shoulder and/or sidewalk. Unlike the other widened structures tested and analyzed in this study, the original section of the slab was doweled and keyed to the new construction. This connection may not be fully effective in transferring transverse bending moments between the new and old portions of the structure, although it will

[3] Wisscasset/ Woolwich No. 2577: Assumption set 3.
[4] Wisscasset/ Woolwich No. 2577: Assumption set 4

effectively transfer shear and could transfer significant longitudinal bending. Consistent with the MaineDOT load ratings and the uncertainty of load transfer across the joint, the initial FE models ignored the new sections of slab and conservatively treated the old portion of the slab as an independent structure. The general condition is shown in Figure 14, with the stelactites indicating the two joints between new/ old/ and new sections.

Figure 14: Penobscot No. 3297 overall configuration with sidewalks and new/ old/ new underneath

The original portion is on average 24.25 ft wide, and has an average thickness of gravel of approximately 17 in on top of the slab and below the asphalt wearing surface. The concrete compressive strength was assumed to be 4 ksi, which corresponds to an elastic modulus of 3600 ksi, likely a reasonable or conservatively higher value.

The finite-element analyses considered the loading caused by the crane moving north in the southbound lane, which produced the largest measured strain of approximately 36 με. Strains were computed assuming isotropic, thin plate theory, which accounts for the effect of both longitudinal and transverse bending moments.

FE model longitudinal strains are reported at the locations of gauges 3060, 3061, 3062, 3072, 3073 and 3074 in Figure 15. The peak model-predicted strain of about 69 με occurred at gauge 3060, which was located nearest the west edge of the slab. Strains tended to steadily decrease across the slab width, with the minimum strain occurring at gauge 3074, which was located closest to the east edge of the slab and furthest away from the applied load. These trends are consistent with observed strains.

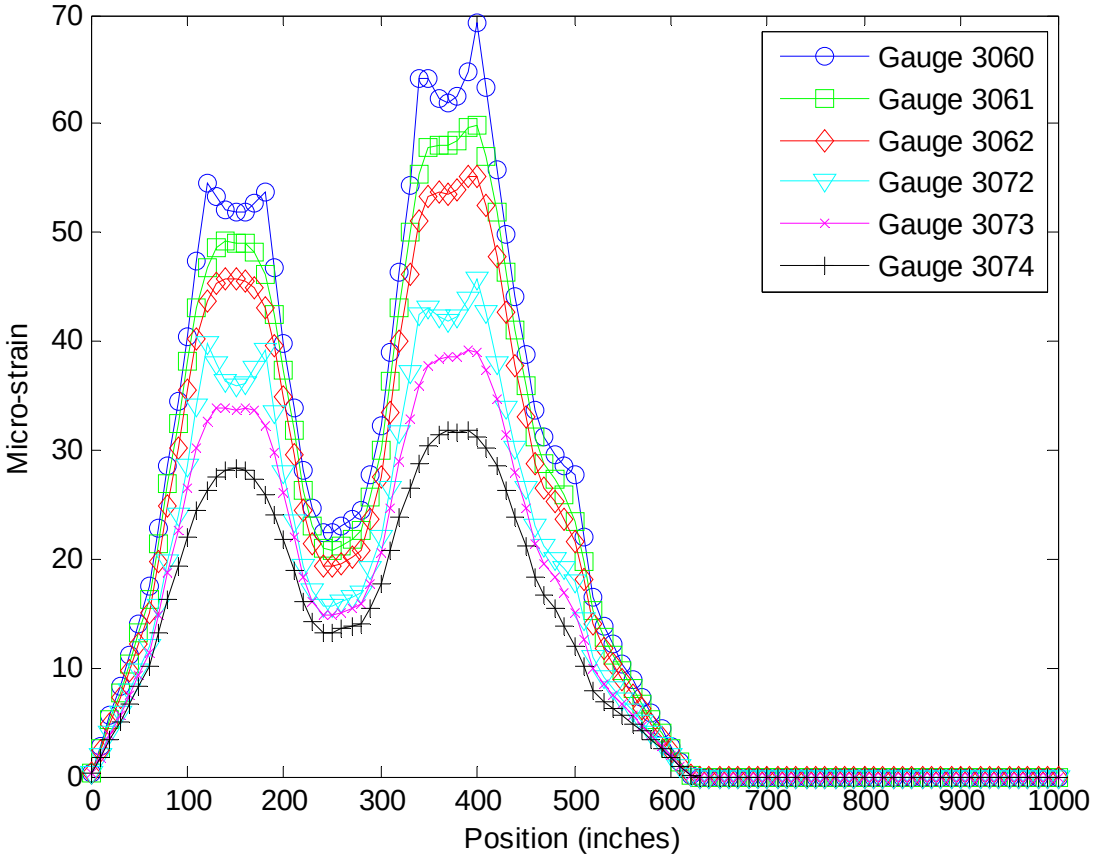

Figure 15: Finite-element predicted strains for Penobscot No. 3297

Table 2 reports peak measured and model-predicted strains, along with the ratio $\varepsilon_c/\varepsilon_T$. The value of $\varepsilon_c/\varepsilon_T$ is quite consistent, ranging from 1.70 to 2.28, and indicates conservatism in the FE model. One driver of this conservatism is likely the presence of an integral curb supported by the newer, approximately 5.4 foot wide section of slab that is keyed and doweled to the older portion. A second cause of conservatism is the significant thickness of fill present under the asphalt, which will tend to spread the wheel load distribution over a wider area of the slab. Finally, the plans call for a concrete wearing surface on the original structure, which was left in place during the widening.

Table 2: Peak measured and model-predicted strains for Penobscot No. 3297

Gauge Location	Peak ε_T (με)	Peak ε_c (με)	$\varepsilon_c/\varepsilon_T$
3060	36.2	69.2	1.91
3061	35.1	59.8	1.70
3062	28.9	55.2	1.91
3072	25.7	45.8	1.78
3073	17.2	39.2	2.28
3074	15.9	31.7	2.00

2.4.2 Revised Load Rating for Penobscot No. 3297

The moment produced with the single crane was approximately 0.66 times that which would be produced by an HL-93 loading including impact and the multiple presence factor of 1.2. This value is less than 0.7, and given the uncertainty of extrapolating measured strains to higher loads, the AASHTO MBE recommends against increasing computed rating factors using the measured strains.

However, the measured strains are quite low. Further, the significant compressive strains measured during the load tests in gauges 3067 and 3071, located at the top of the curbs indicate that the doweled and keyed joints between the original and widened portions of the slab do result in the slab behaving more like a single unit, and the new, widened portions and curbs were mobilized during live loading. Finally, the existing concrete wearing surface on the older structure, with a thickness tapering from 3 inches at the curb to 5 inches at the roadway crown, may increase the effective slab thickness.

In light of these observations, an independent load rating was conducted by the University of Maine using *SlabRate* given the following assumptions:

1. Weights, slab dimensions, and wearing surface loads were estimated per the widening plans. The slab span was taken as the clear span of 20 feet.
2. The structure was assumed to be the full 40.67 feet wide with two 12 foot lanes and 6.33 foot wide sidewalk sections on each side, which is equivalent to assuming that the doweled, keyed joint fully transferred all moment and shear.
3. Wheel loads were allowed within two feet from the sidewalk edge (8.333 ft from the slab edge).
4. The slab thickness was taken as the structural thickness of 16 inches plus the 3 inch wearing surface at the edge of the original slab for a total of 19 inches.
5. An average thickness of fill of 17 inches weighing 140 pcf was assumed to exist between the curbs along with 3 inches of asphalt at 145 pcf. The curb weight was taken as 667 lb/lf for the cast concrete, and the railing was assumed as 200 lb/lf.
6. The sidewalk weights were added as separate line loads assuming 30 in deep by 60 in wide fill sections with a 3 in thick by 60 in wide asphalt wearing surfaces.
7. The stiffness of the thickened curbs was conservatively not accounted for in the analysis.
8. The reinforcing was 1.8 in^2/ft per the original plans, with a yield strength of 33 ksi.
9. The wheel loads were distributed over 27 inch long by 37 inch wide patches, a 17 inch increase in the normal 10 inch by 20 inch dimension specified by AASHTO to account for the distribution of load through the fill.

Given these assumptions, the operating rating factors for two lanes of HL-93 loading is 1.34[5]. This value is the minimum that occurs at mid-span of the original slab near the edge of the

[5] Penobscot No. 3297: Assumption set 1.

sidewalk (node 207 in the finite-element model), and was accessed from the *SlabRate* results independently of the user interface. It is important to note that the widened portions of the slab are 16 inches thick with no wearing surface, which is not consistent with the assumption of a 19 inch thick slab. However, this reduced thickness is compensated for by the larger amount of reinforcing (2 in^2/ft) and higher grade of reinforcing (Gr 60) in the newer, widened portions. A parallel *SlabRate* analysis assuming a 16 inch slab with reinforcing corresponding to the newer construction indicates that the widened portions has an HL-93 operating rating factor of 2.43[6].

These rating factors indicate that the Penobscot Bridge No 3297 may be structurally sufficient. However, the single most important assumption leading to an increase in rating factors is that the effective slab thickness is 19 inches, i.e. that the wearing surface called out on the plans can be added to the structural thickness of 16 inches. Indeed, a parallel rating analysis assuming a slab thickness of 16 inches gives an operating rating factor of 0.76 for two lanes of HL-93 loading[7]. Given that the wearing surface cannot be inspected, and that demolition of the original curbs is called for on the as-built plans near the edge of the original slab, this assumption could be unconservative. We recommend that the MaineDOT carefully consider all assumptions inherent in the rating analysis described here when assessing the capacity of this structure.

2.5 FE Analysis of Smyrna No. 2250 and Comparison with Field Data

The Smyrna bridge consists of an original section and widened portions at both edges. The original portion of the structure represents approximately 70% of the roadway width between the curbs, and only the new portion on the north (upstream) side carries significant traffic. The general condition is shown in Figure 16 focused on a joint between old and new slabs.

Figure 16: Smyrna No. 2250 underside general condition with joint detail

[6] Penobscot No. 3297: Assumption set 2.
[7] Penobscot No. 3297: Assumption set 3.

During the live load tests, the truck was consistently driven close to each curb. As a result, the original portion of the slab was not loaded by both wheel lines of the truck. The widened portion on the north side, however, did carry one full lane of traffic. The truck positioning is reflected in the measured strains, for which the maximum value was 43.9 με in the northern, widened portion and 25.3 με in the thicker, more lightly loaded original portion of the slab.

Because of this, the analysis focused on the new portion of the structure. The clear span of 20 feet was used in the analyses, along with the average width of 17 ft 8 inches. The slab thickness was taken as 16.5 inches as specified on the plans. As for all other structures, the slab was considered uncracked, and a 20 x 20 finite-element mesh was used. Figure 17 shows the model-predicted strains at the four gauges located nearest the truck wheel lines on the bottom of the slab, and Table 3 summarizes peak measured and model-predicted strains at the four gage locations.

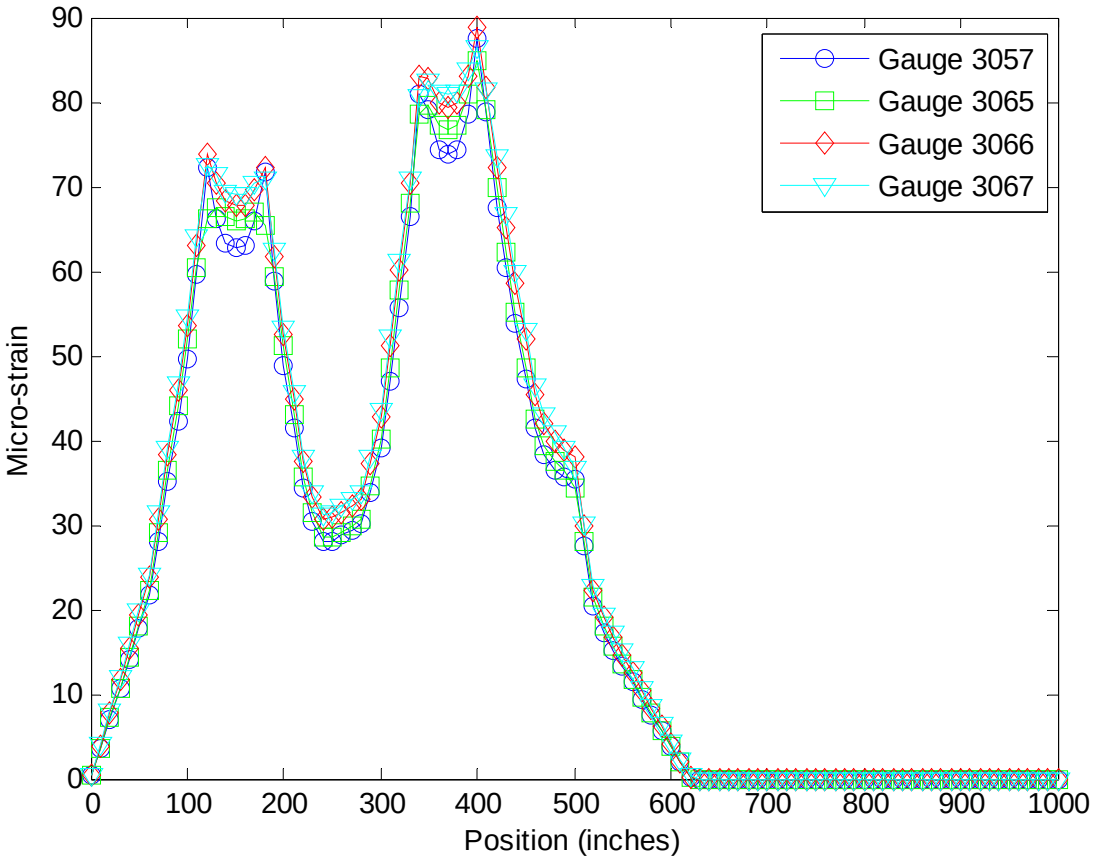

Figure 17: Finite-element predicted strains for Smyrna No. 2250

Table 3: Peak measured and model-predicted strains for Smyrna No. 2250

Gauge Location	Peak ε_T (με)	Peak ε_c (με)	$\varepsilon_c/\varepsilon_T$
3057	23.9	87.4	3.66
3065	27.0	84.8	3.14
3066	43.9	88.7	2.02
3067	25.5	86.6	3.39

Three of the four gauges had very similar strains, but at gauge 3066 the measured strain was significantly larger. This contrasts with the finite-element model predictions, which are similar at all gauge locations. The minimum ratio of computed to predicted strain is 2.02 at the location of gauge 3066. However, the maximum moment produced by the truck was less than 0.7 times an HL-93 live load with impact, and therefore the measured strains cannot be used directly to revise the rating factor.

A.1 Weld No. 5361

A.1.1 Instrumentation

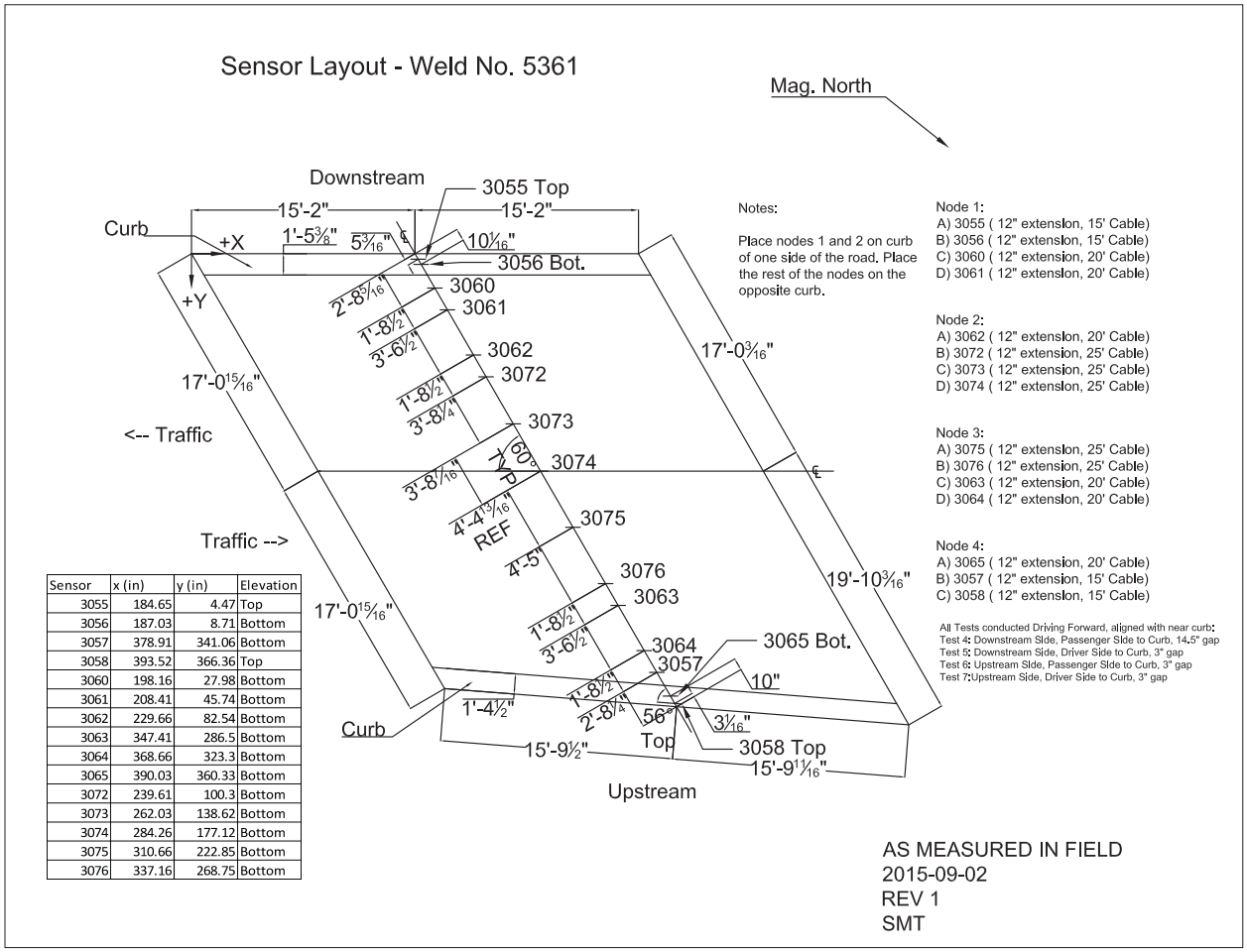

Sensor	x (in)	y (in)	Elevation
3055	184.65	4.47	Top
3056	187.03	8.71	Bottom
3057	378.91	341.06	Bottom
3058	393.52	366.36	Top
3060	198.16	27.98	Bottom
3061	208.41	45.74	Bottom
3062	229.66	82.54	Bottom
3063	347.41	286.5	Bottom
3064	368.66	323.3	Bottom
3065	390.03	360.33	Bottom
3072	239.61	100.3	Bottom
3073	262.03	138.62	Bottom
3074	284.26	177.12	Bottom
3075	310.66	222.85	Bottom
3076	337.16	268.75	Bottom

Figure 18: Weld No. 5361 sensor layout

A.1.2 Loading

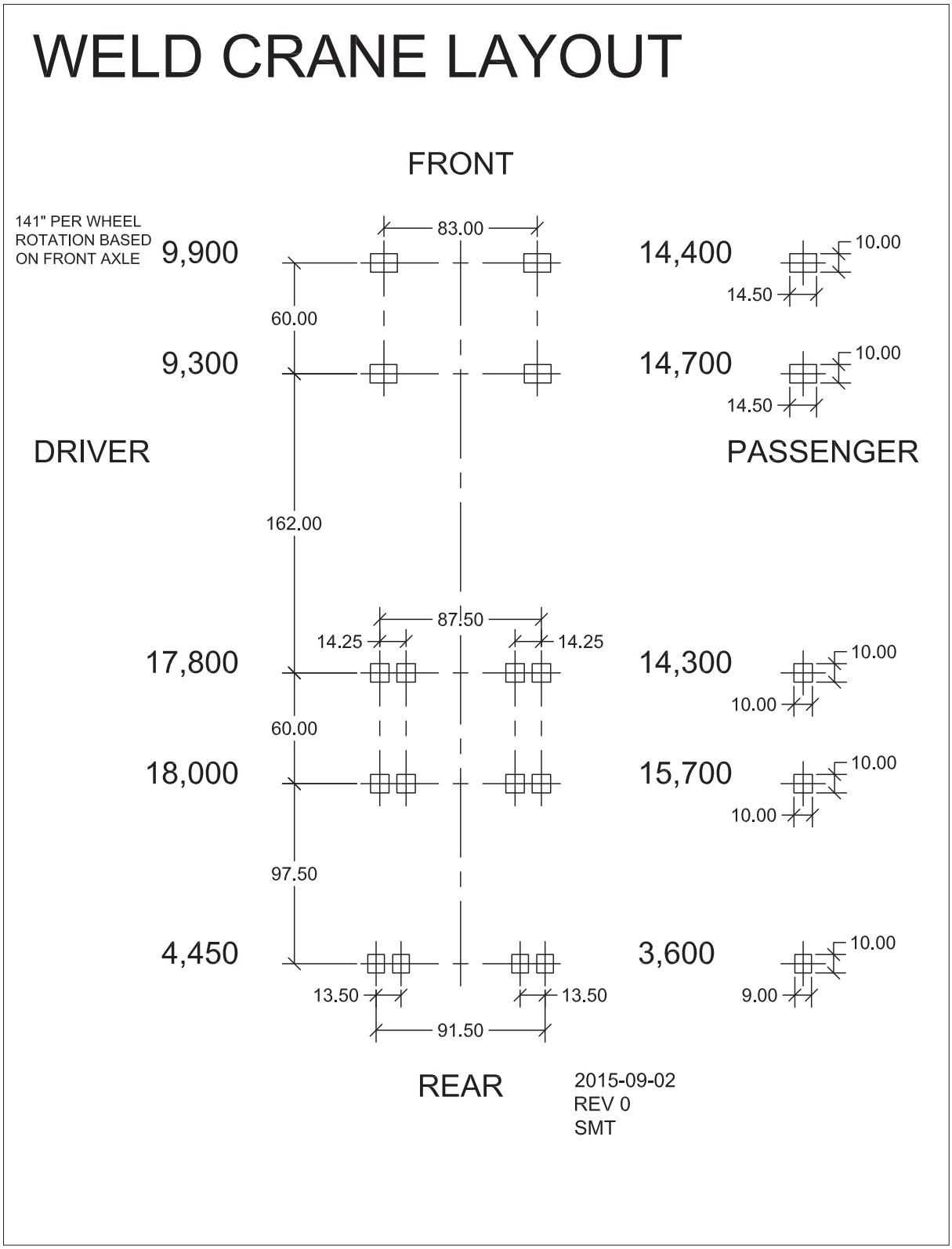

Figure 19: Weld No. 5361 crane layout

A.1.3 Representative Data Plots

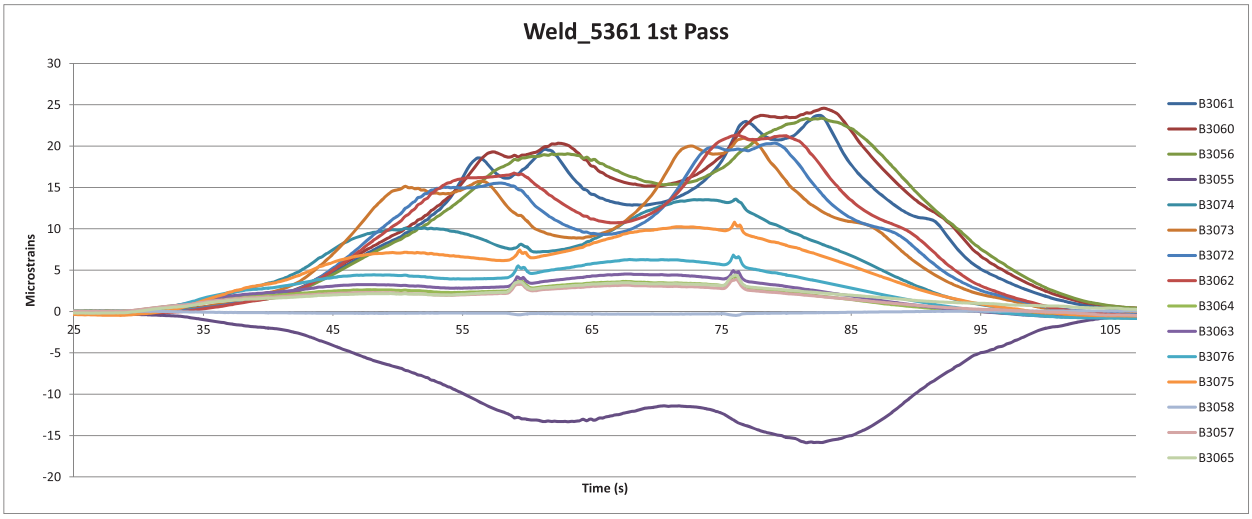

Figure 20: Weld No. 5361 test 4, 1st pass

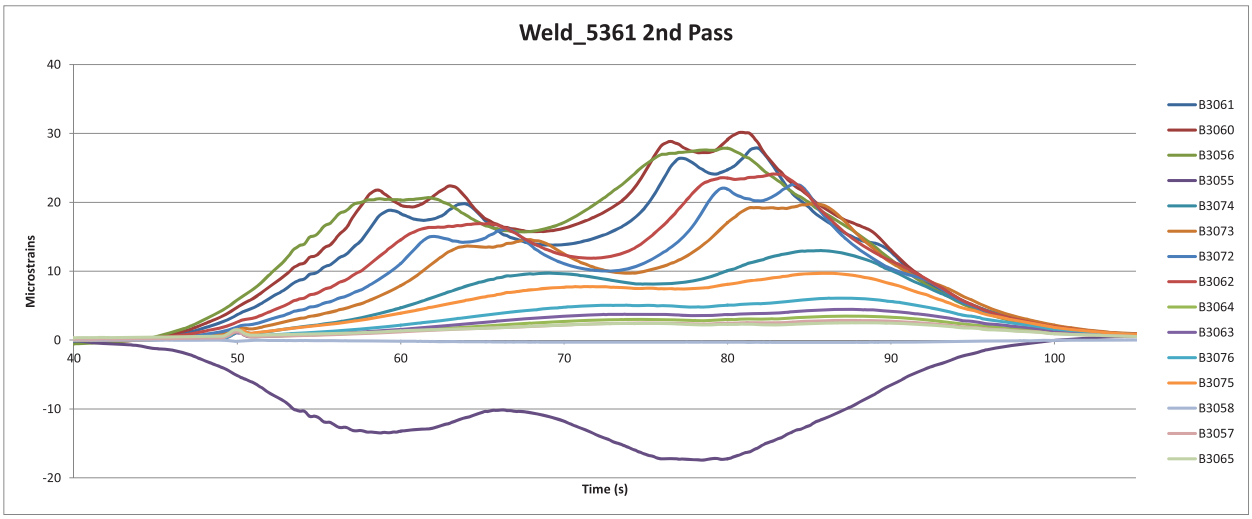

Figure 21: Weld No. 5361 test 5, 2nd pass

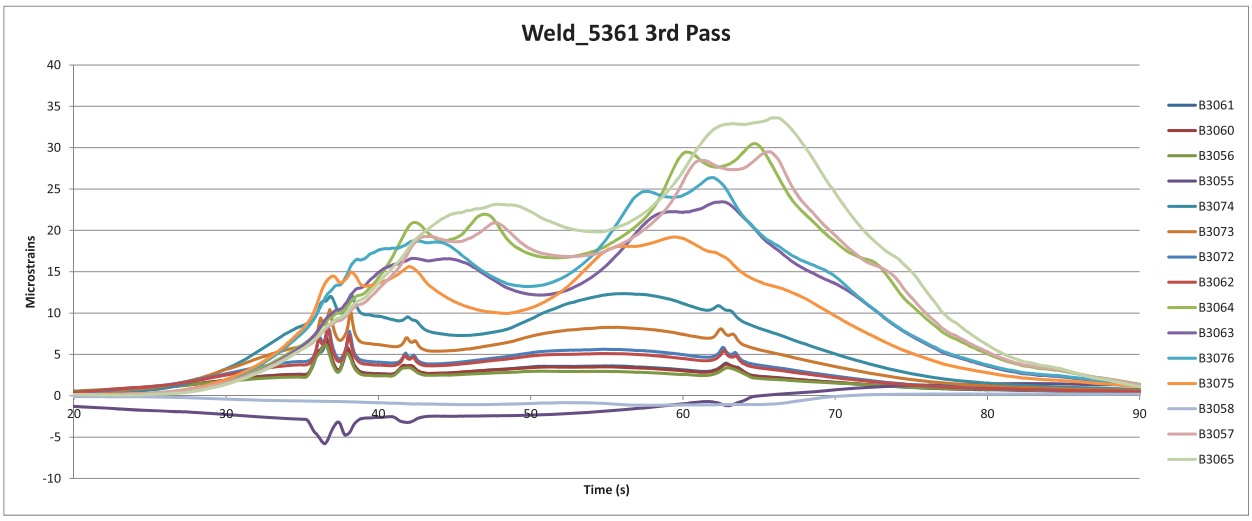

Figure 22: Weld No. 5361 test 6, 3rd pass

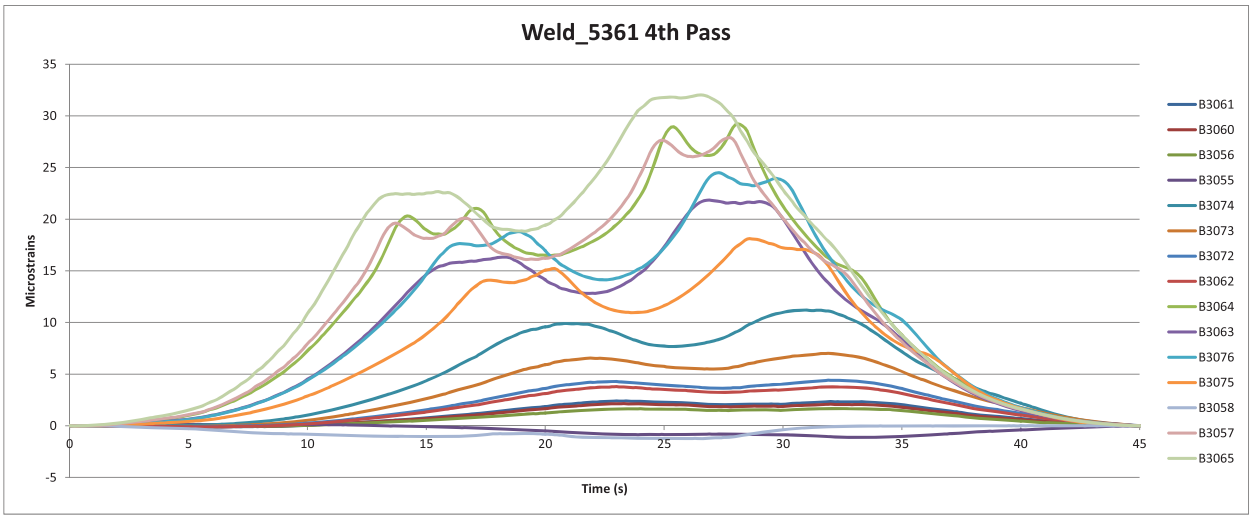

Figure 23: Weld No. 5361 test 7, 4th pass

A.2 West Paris No. 2582

A.2.1 Instrumentation

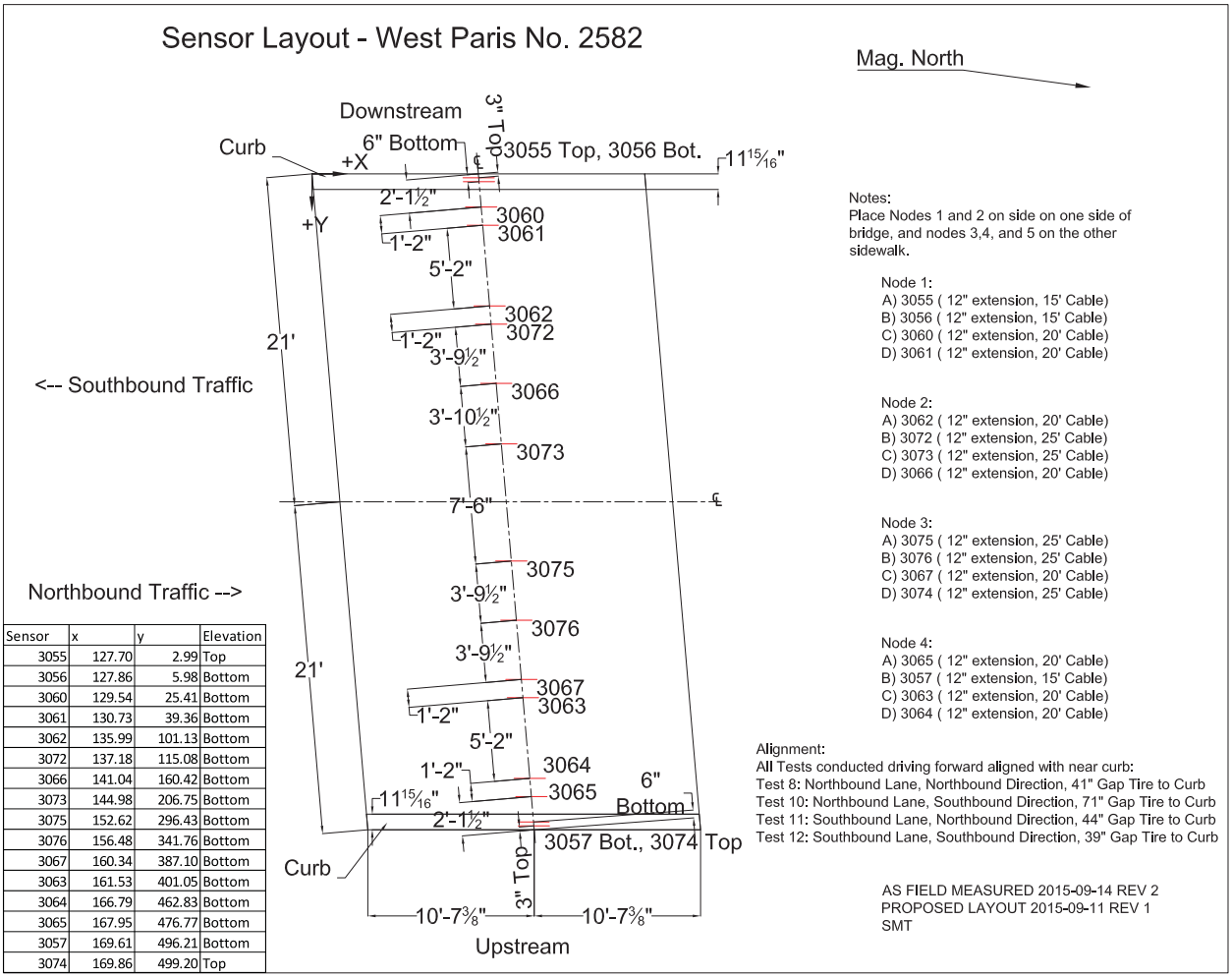

Sensor	x	y	Elevation
3055	127.70	2.99	Top
3056	127.86	5.98	Bottom
3060	129.54	25.41	Bottom
3061	130.73	39.36	Bottom
3062	135.99	101.13	Bottom
3072	137.18	115.08	Bottom
3066	141.04	160.42	Bottom
3073	144.98	206.75	Bottom
3075	152.62	296.43	Bottom
3076	156.48	341.76	Bottom
3067	160.34	387.10	Bottom
3063	161.53	401.05	Bottom
3064	166.79	462.83	Bottom
3065	167.95	476.77	Bottom
3057	169.61	496.21	Bottom
3074	169.86	499.20	Top

Figure 24: West Paris No. 2582 sensor layout

A.2.2 Loading

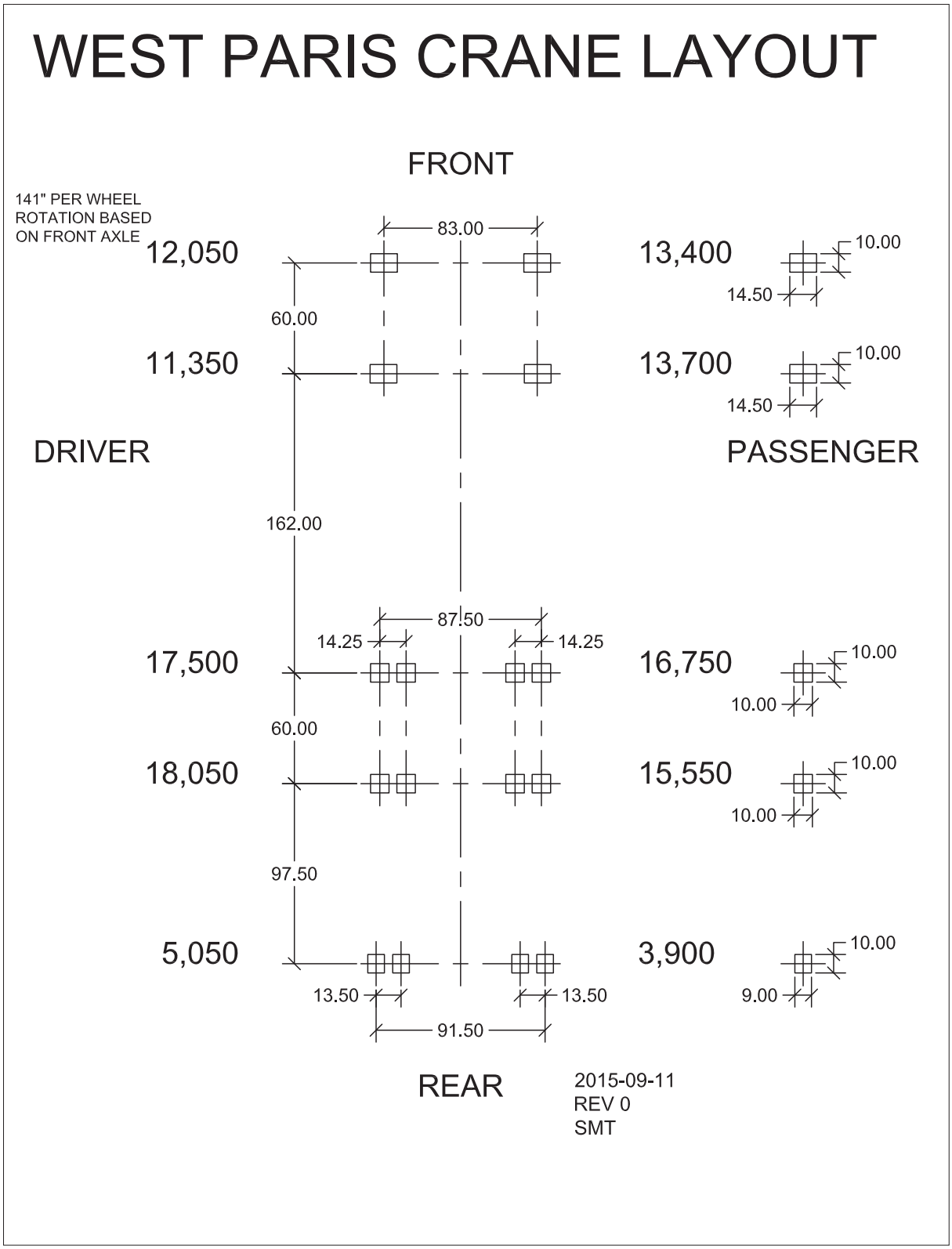

Figure 25: West Paris No. 2582 crane layout

A.2.3 Representative Data Plots

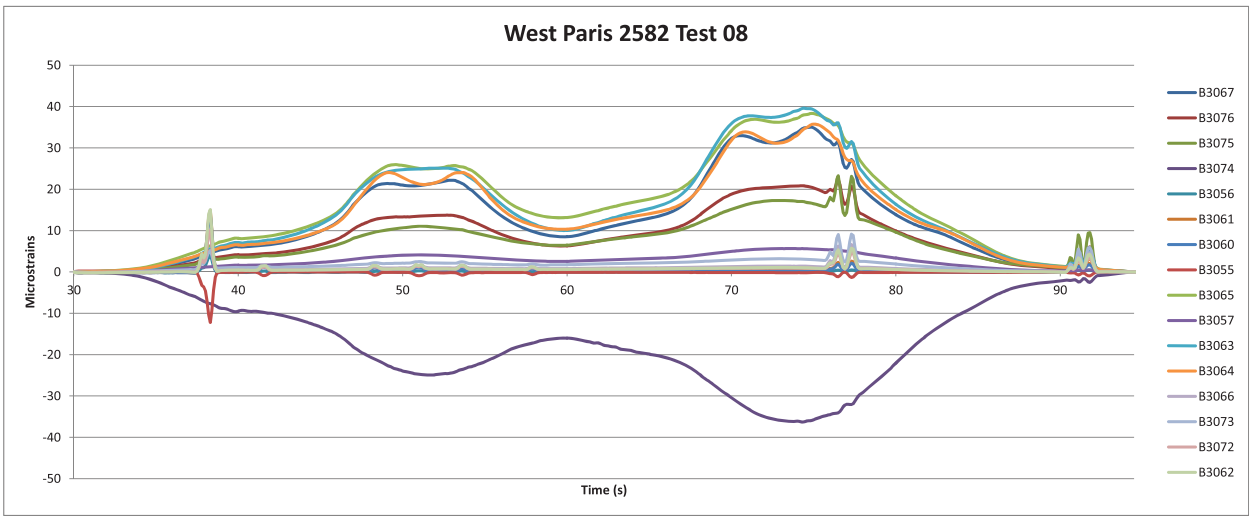

Figure 26: West Paris No. 2582, test 8

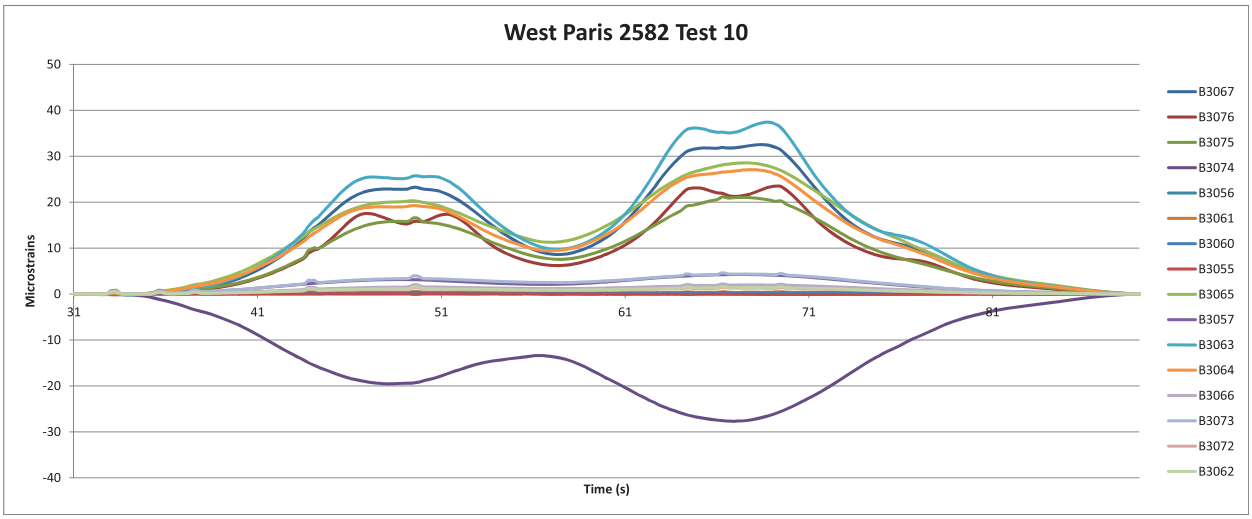

Figure 27: West Paris No. 2582, test 10

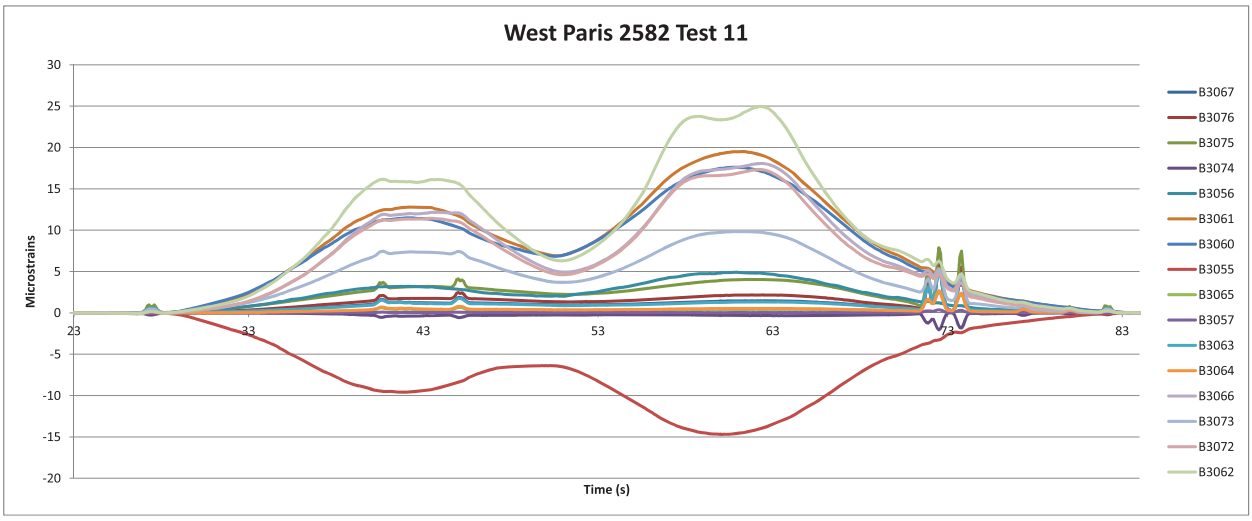

Figure 28: West Paris No. 2582, test 11

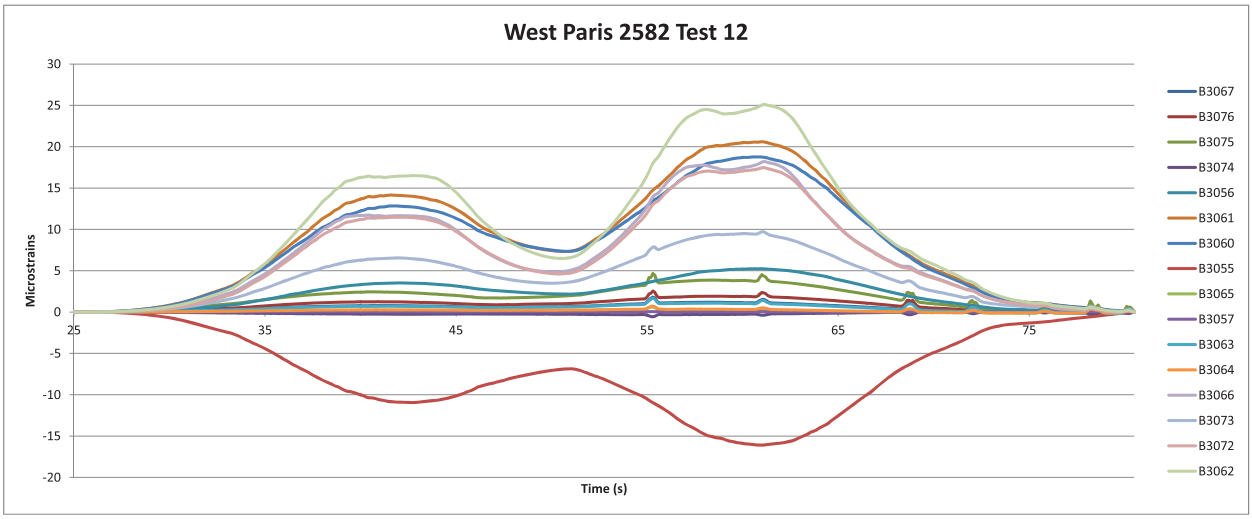

Figure 29: West Paris No. 2582, test 12

A.3 Woolwich No. 2577

A.3.1 Instrumentation

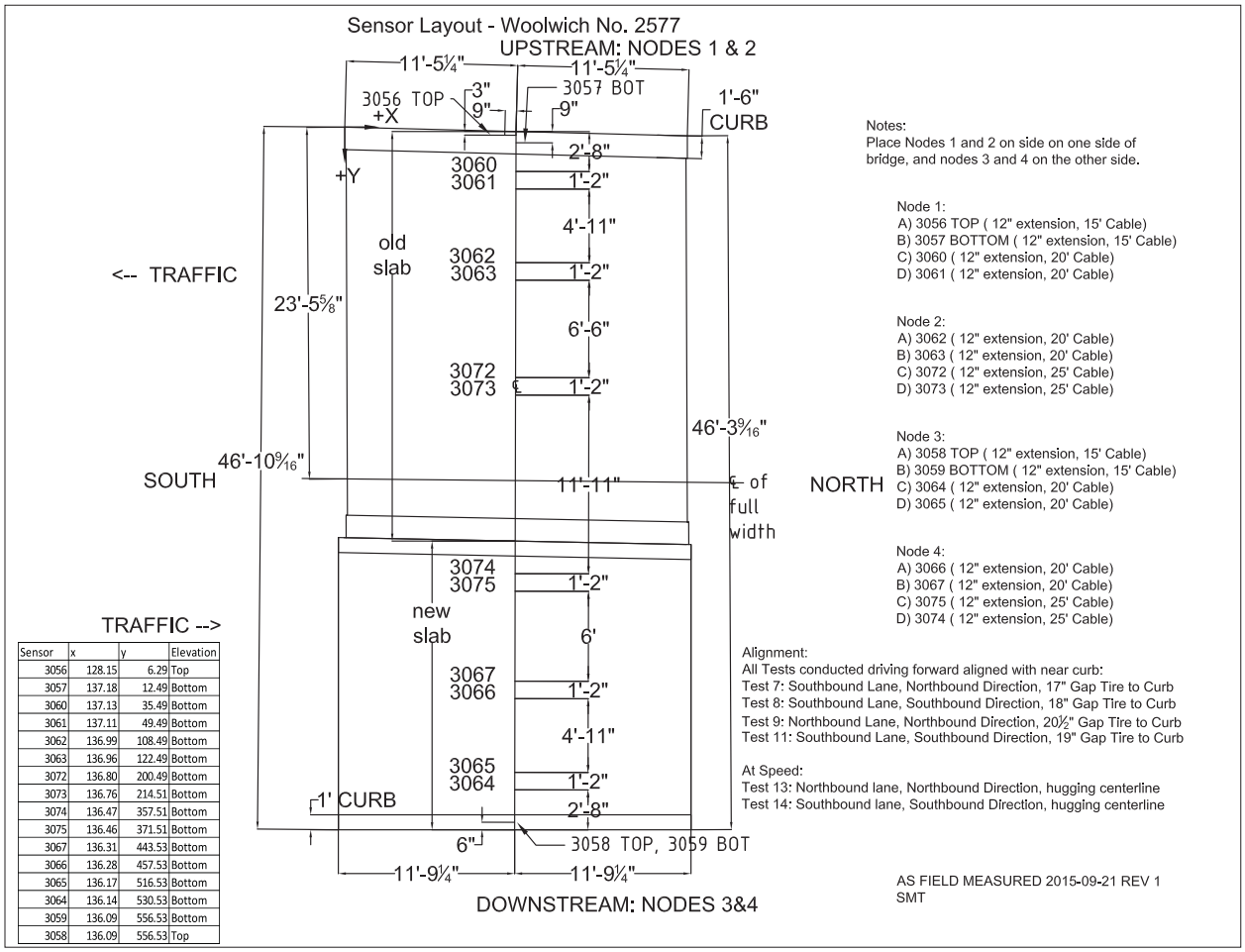

Sensor	x	y	Elevation
3056	128.15	6.29	Top
3057	137.18	12.49	Bottom
3060	137.13	35.49	Bottom
3061	137.11	49.49	Bottom
3062	136.99	108.49	Bottom
3063	136.96	122.49	Bottom
3072	136.80	200.49	Bottom
3073	136.76	214.51	Bottom
3074	136.47	357.51	Bottom
3075	136.46	371.51	Bottom
3067	136.31	443.53	Bottom
3066	136.28	457.53	Bottom
3065	136.17	516.53	Bottom
3064	136.14	530.53	Bottom
3059	136.09	556.53	Bottom
3058	136.09	556.53	Top

Figure 30: Woolwich No. 2577 sensor layout

A.3.2 Loading

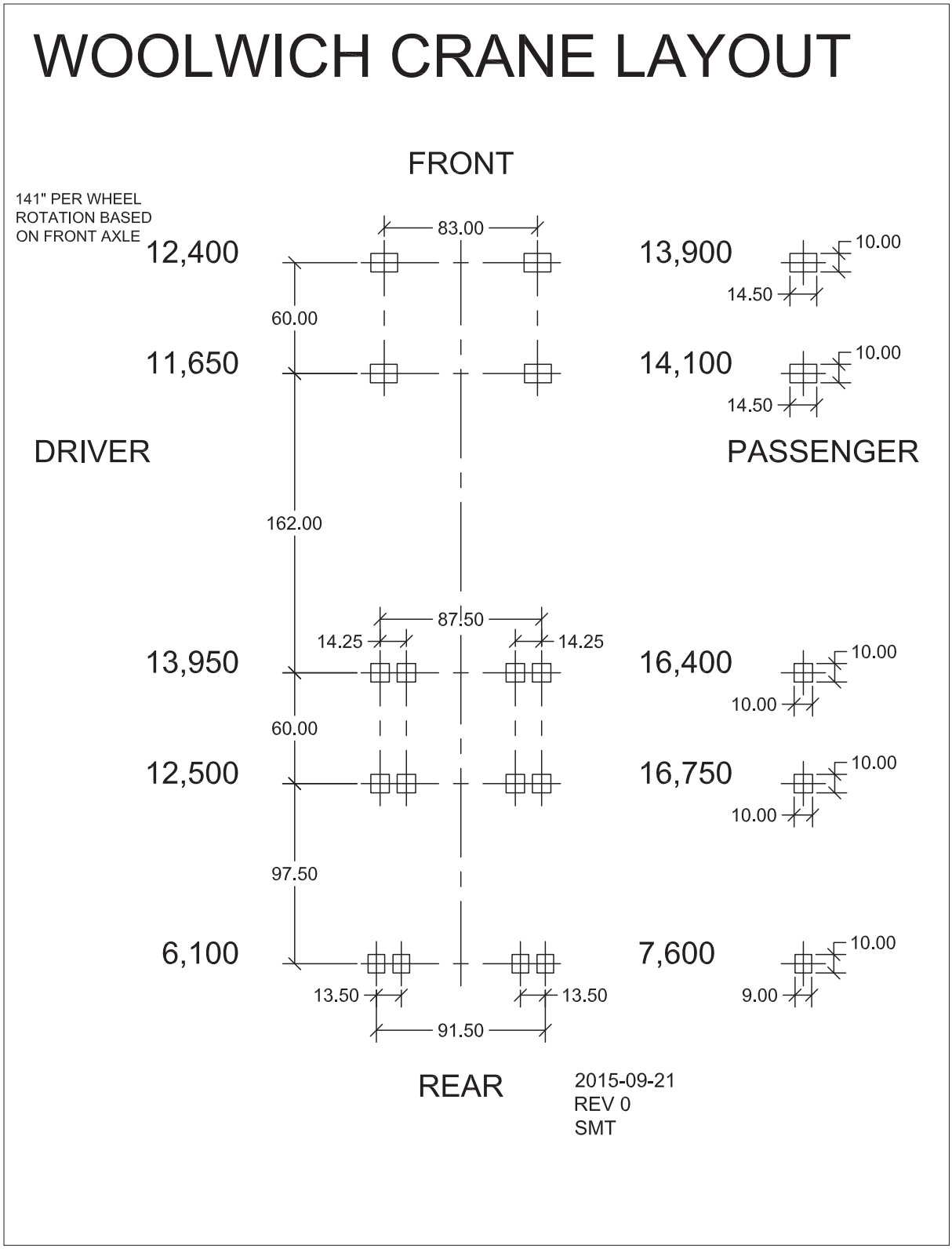

Figure 31: Woolwich No. 2577 crane layout

A.3.3 Representative Data Plots

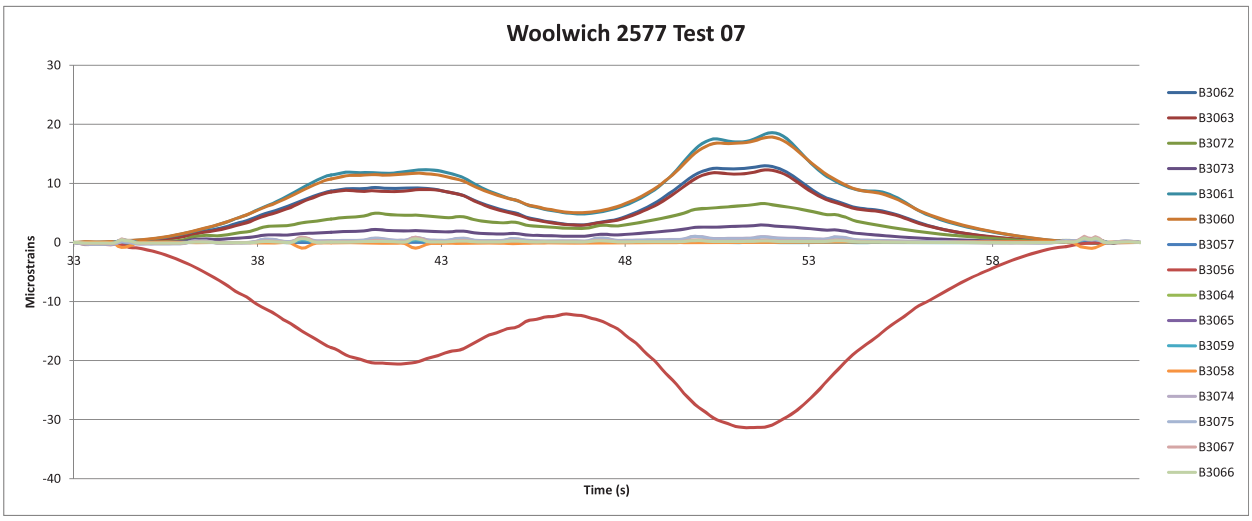

Figure 32: Woolwich No. 2577, test 7

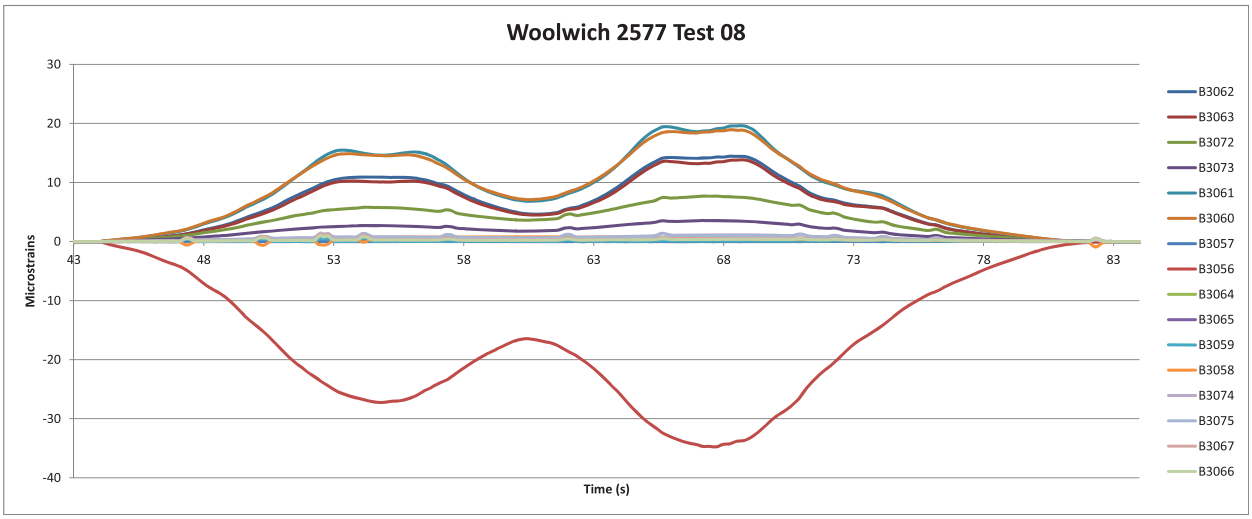

Figure 33: Woolwich No. 2577, test 8

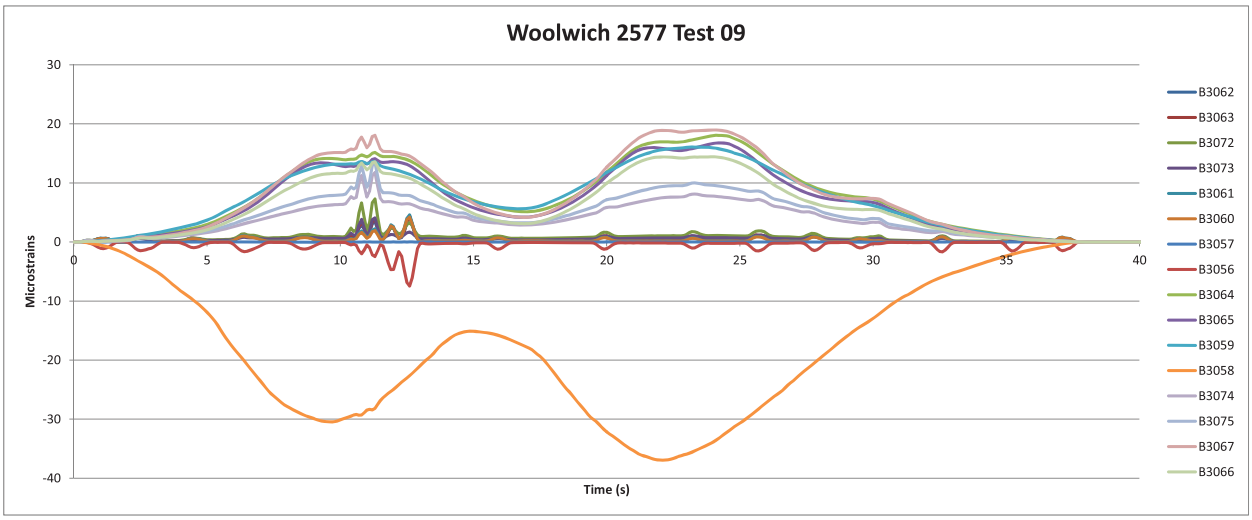

Figure 34: Woolwich No. 2577, test 9

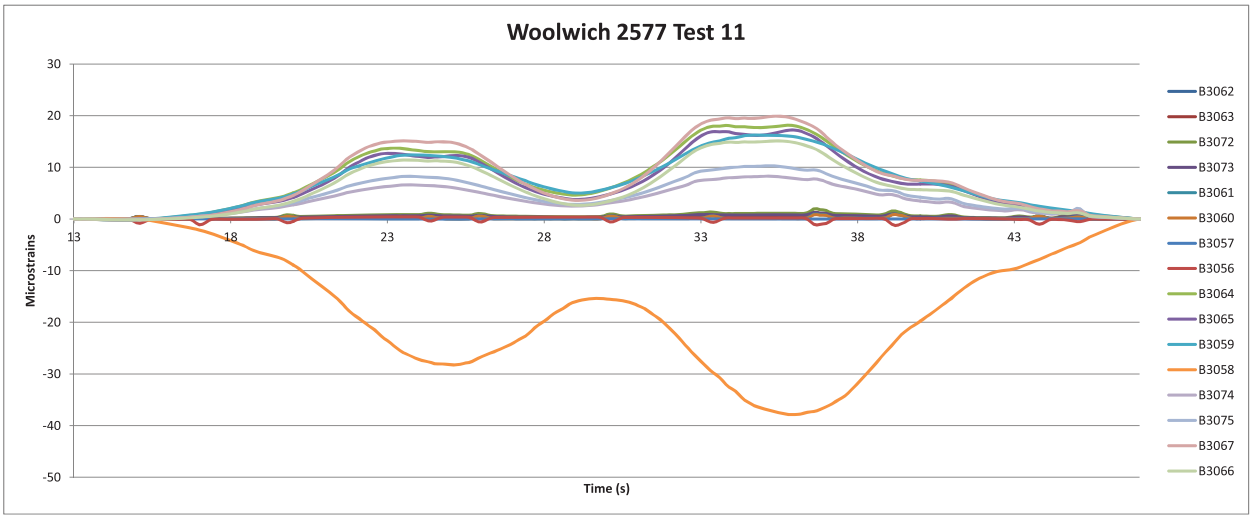

Figure 35: Woolwich No. 2577, test 11

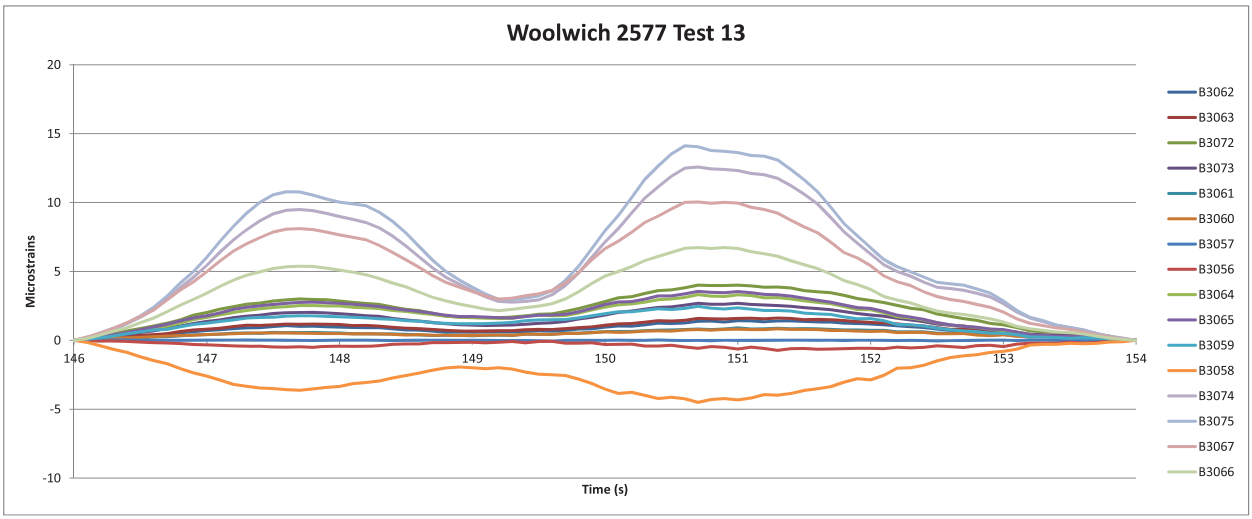

Figure 36: Woolwich No. 2577, test 13

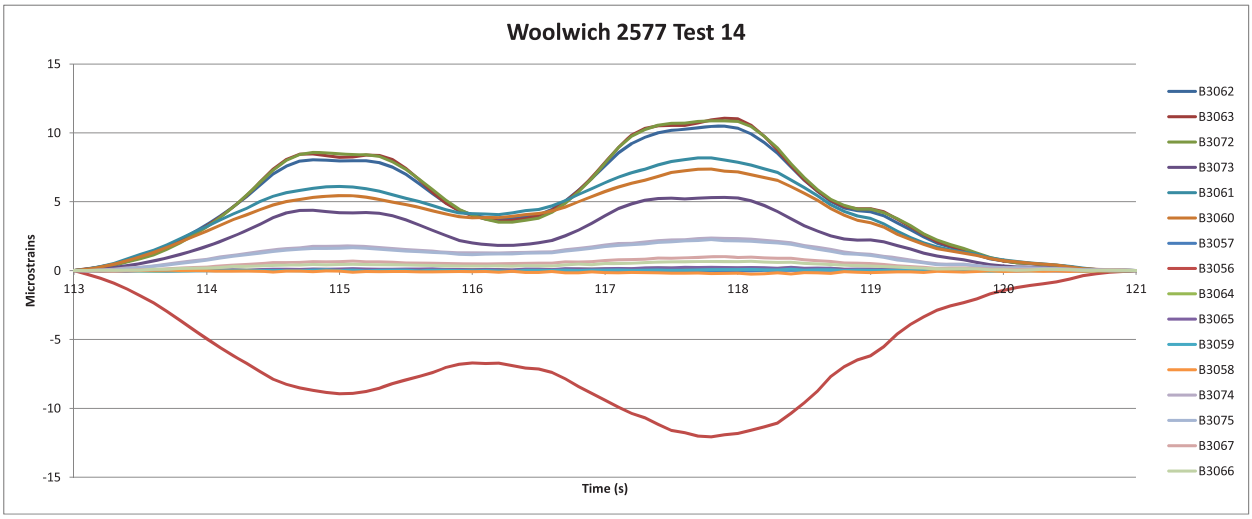

Figure 37: Woolwich No. 2577, test 14

A.4 Penobscot No. 3297

A.4.1 Instrumentation

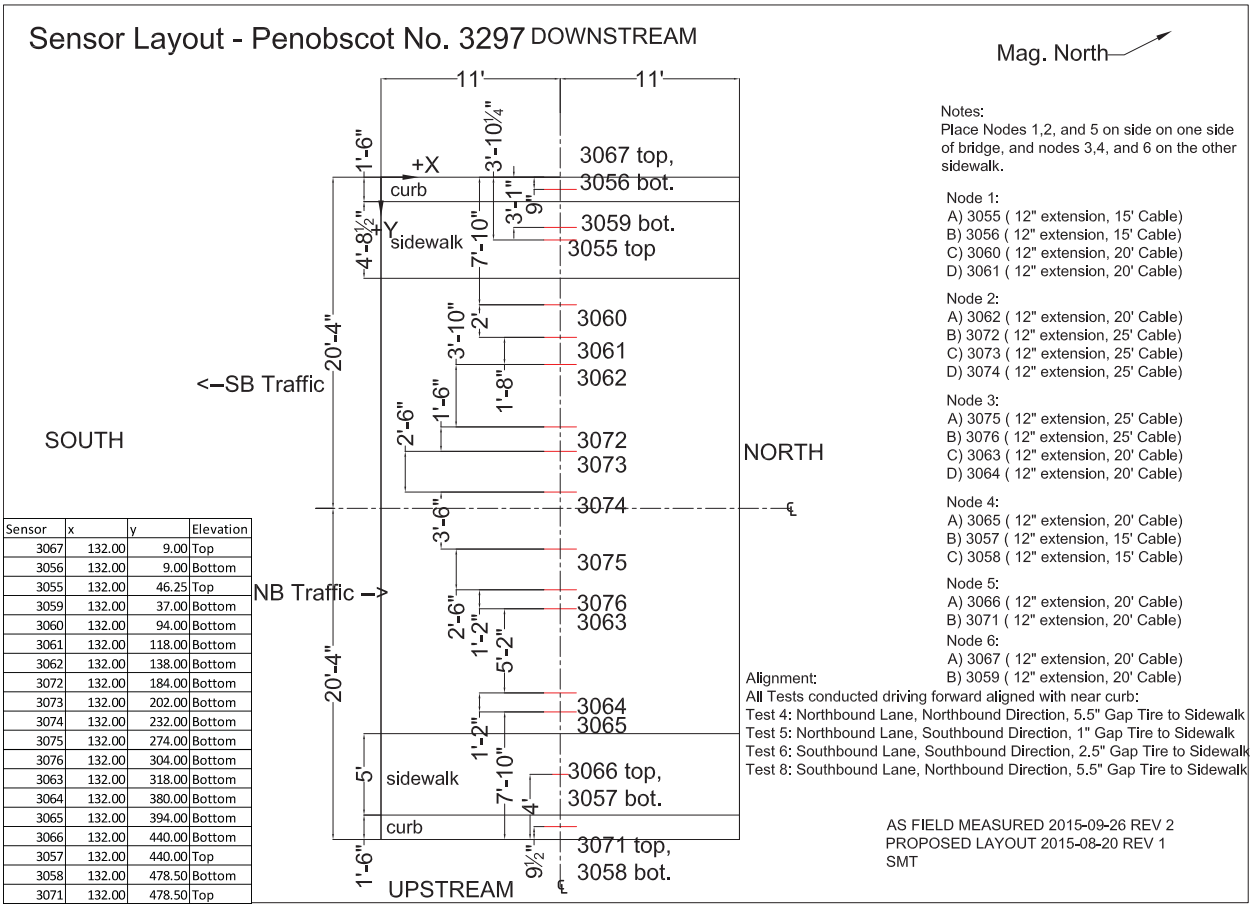

Sensor	x	y	Elevation
3067	132.00	9.00	Top
3056	132.00	9.00	Bottom
3055	132.00	46.25	Top
3059	132.00	37.00	Bottom
3060	132.00	94.00	Bottom
3061	132.00	118.00	Bottom
3062	132.00	138.00	Bottom
3072	132.00	184.00	Bottom
3073	132.00	202.00	Bottom
3074	132.00	232.00	Bottom
3075	132.00	274.00	Bottom
3076	132.00	304.00	Bottom
3063	132.00	318.00	Bottom
3064	132.00	380.00	Bottom
3065	132.00	394.00	Bottom
3066	132.00	440.00	Bottom
3057	132.00	440.00	Top
3058	132.00	478.50	Bottom
3071	132.00	478.50	Top

Figure 38: Penobscot No. 3297 sensor layout

A.4.2 Loading

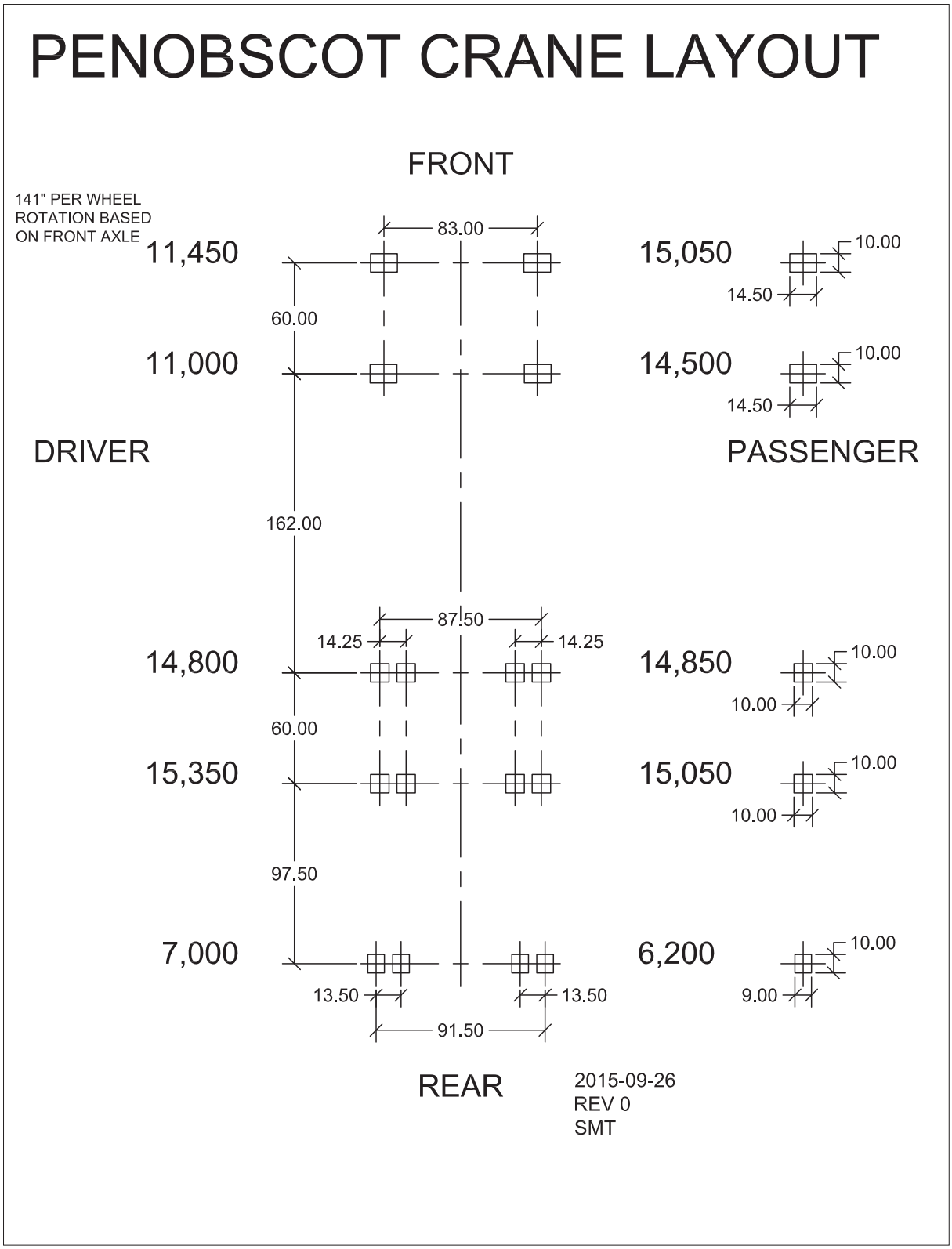

Figure 39: Penobscot No. 3297 crane layout

A.4.3 Representative Data Plots

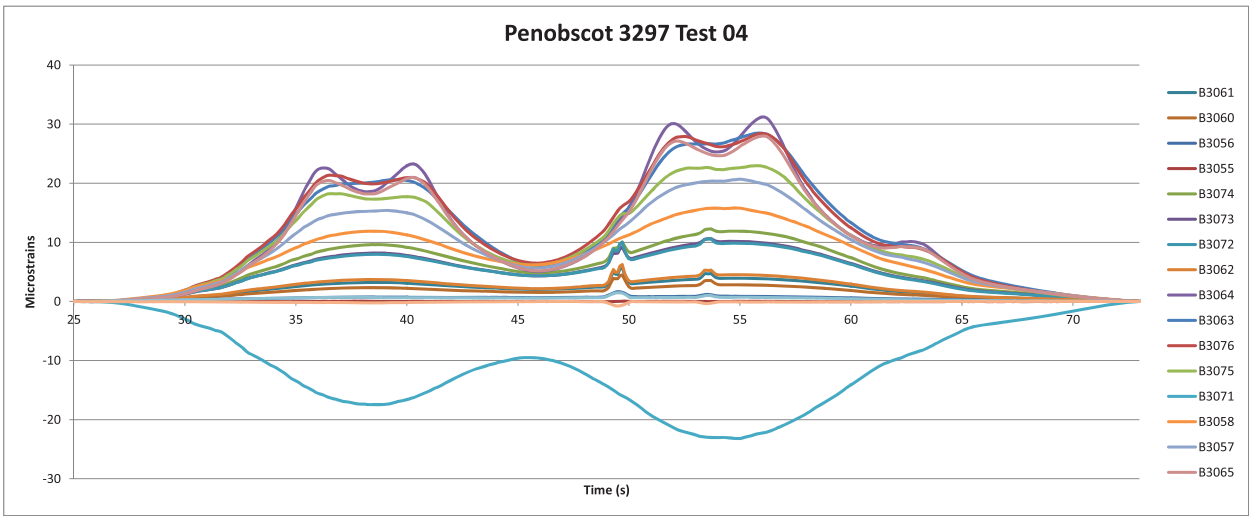

Figure 40: Penobscot No. 3297, test 4

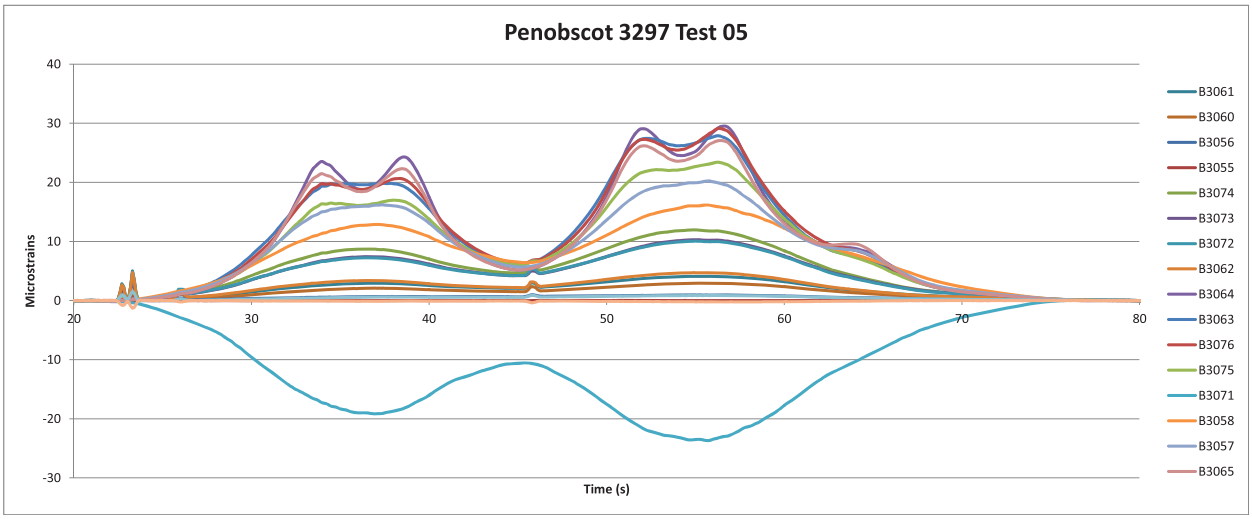

Figure 41: Penobscot No. 3297, test 5

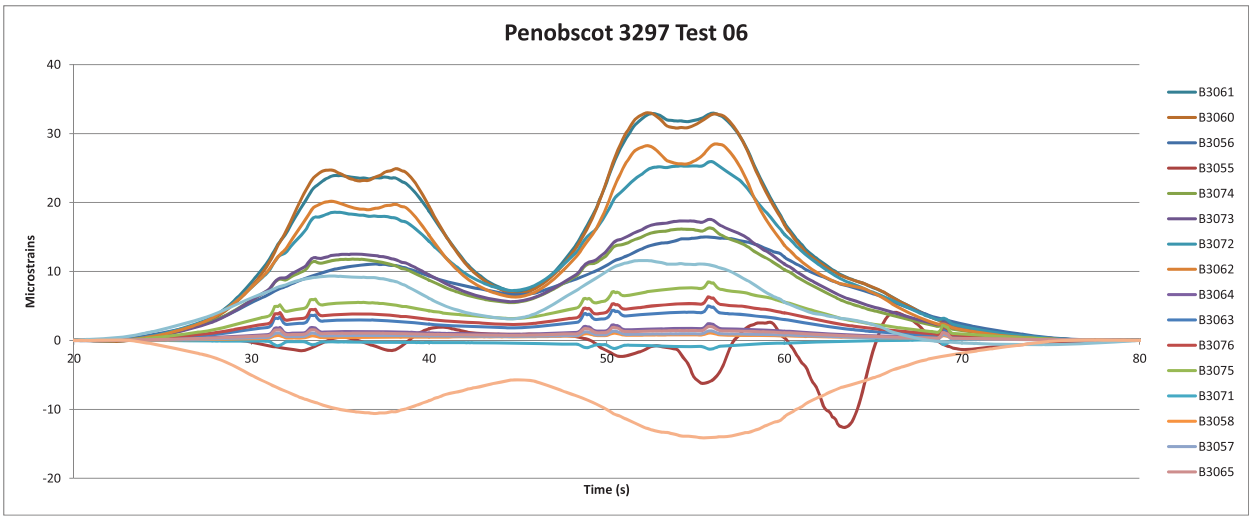

Figure 42: Penobscot No. 3297, test 6

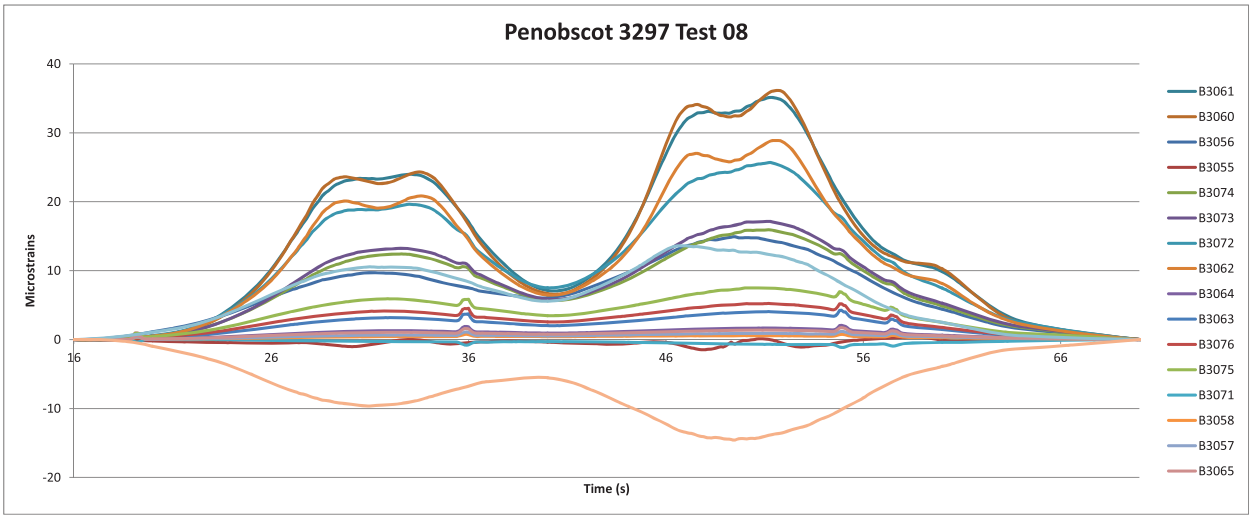

Figure 43: Penobscot No. 3297, test 8

A.5 Smyrna No. 2250

A.5.1 Instrumentation

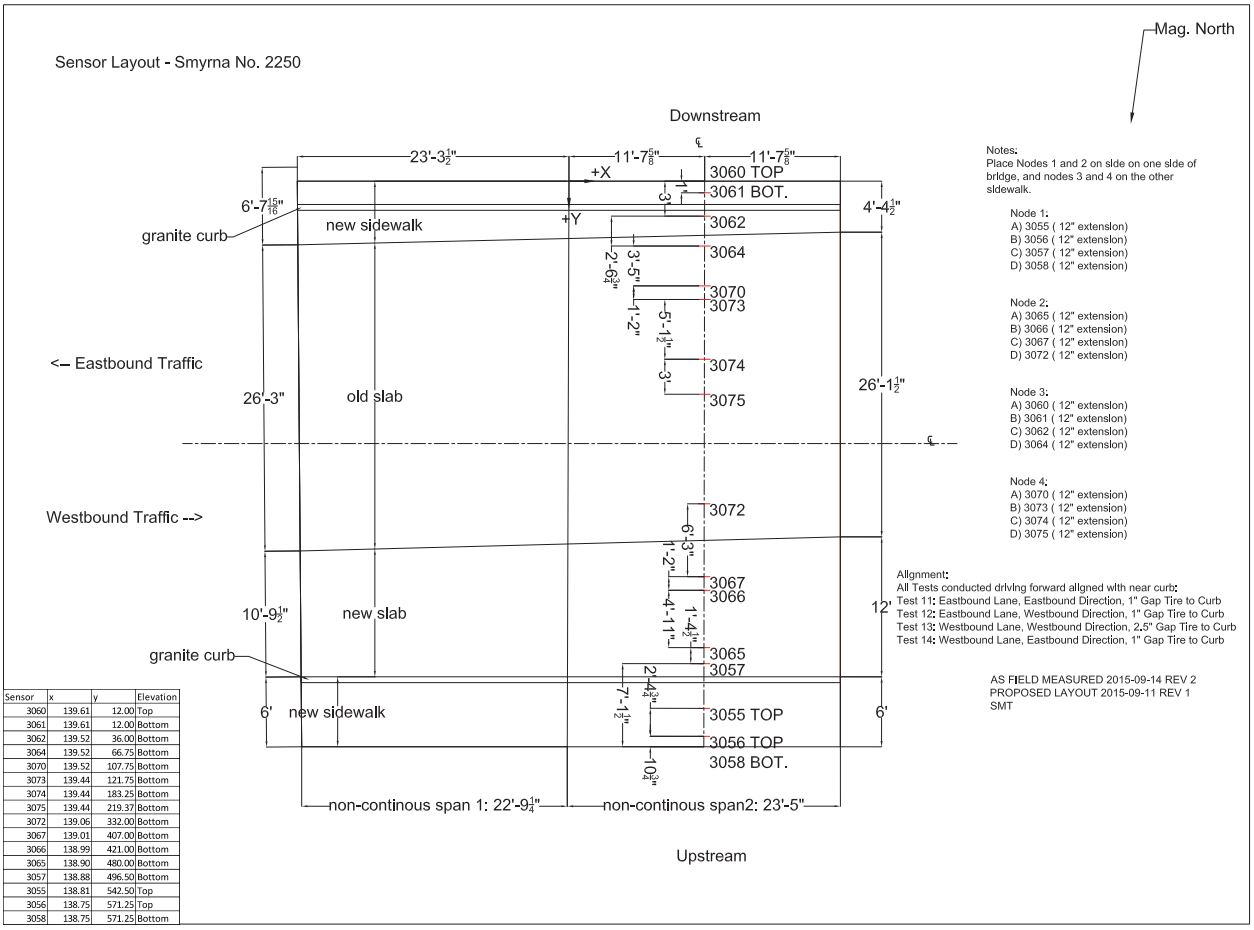

Sensor	x	y	Elevation
3060	139.61	12.00	Top
3061	139.61	12.00	Bottom
3062	139.52	36.00	Bottom
3064	139.52	66.75	Bottom
3070	139.52	107.75	Bottom
3073	139.44	121.75	Bottom
3074	139.44	183.25	Bottom
3075	139.44	219.37	Bottom
3072	139.06	332.00	Bottom
3067	139.01	407.00	Bottom
3066	138.99	421.00	Bottom
3065	138.90	480.00	Bottom
3057	138.88	496.50	Bottom
3055	138.81	542.50	Top
3056	138.75	571.25	Top
3058	138.75	571.25	Bottom

Figure 44: Smyrna No. 2250 sensor layout

A.5.2 Loading

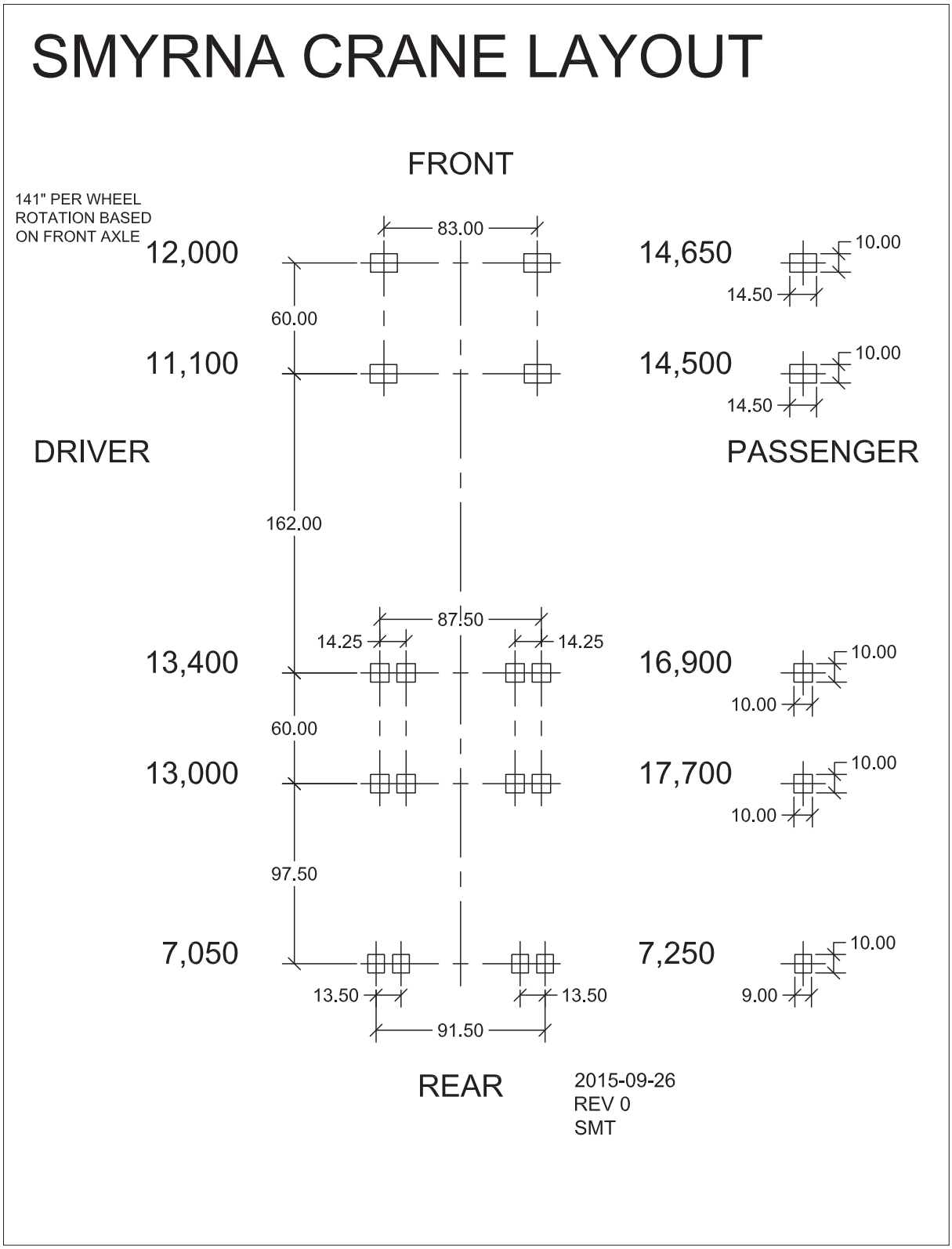

Figure 45: Symyrna No. 2250 crane layout

A.5.3 Representative Data Plots

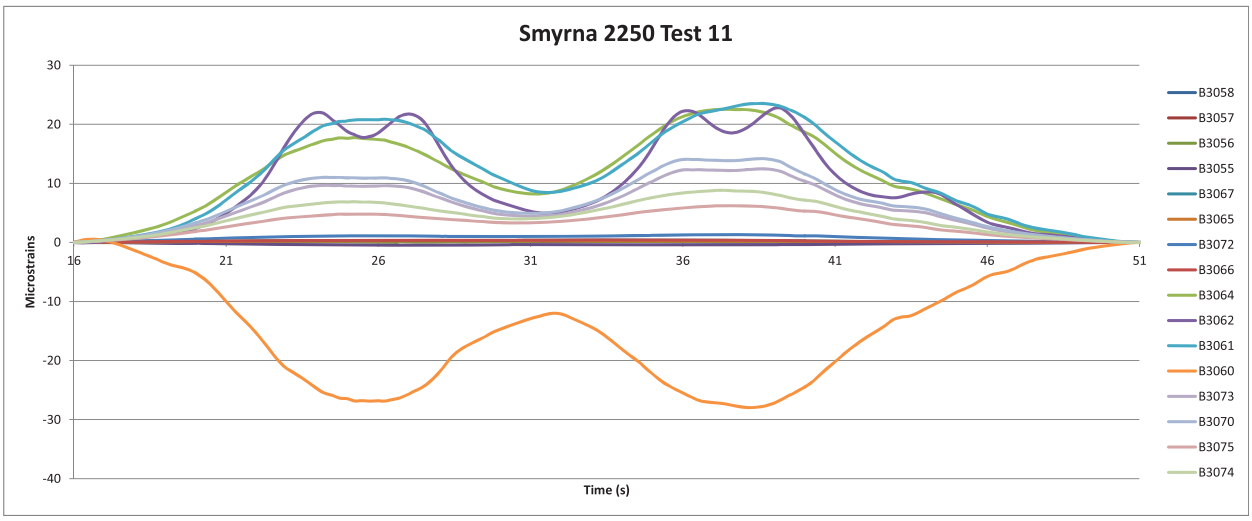

Figure 46: Smyrna 2250, test 11

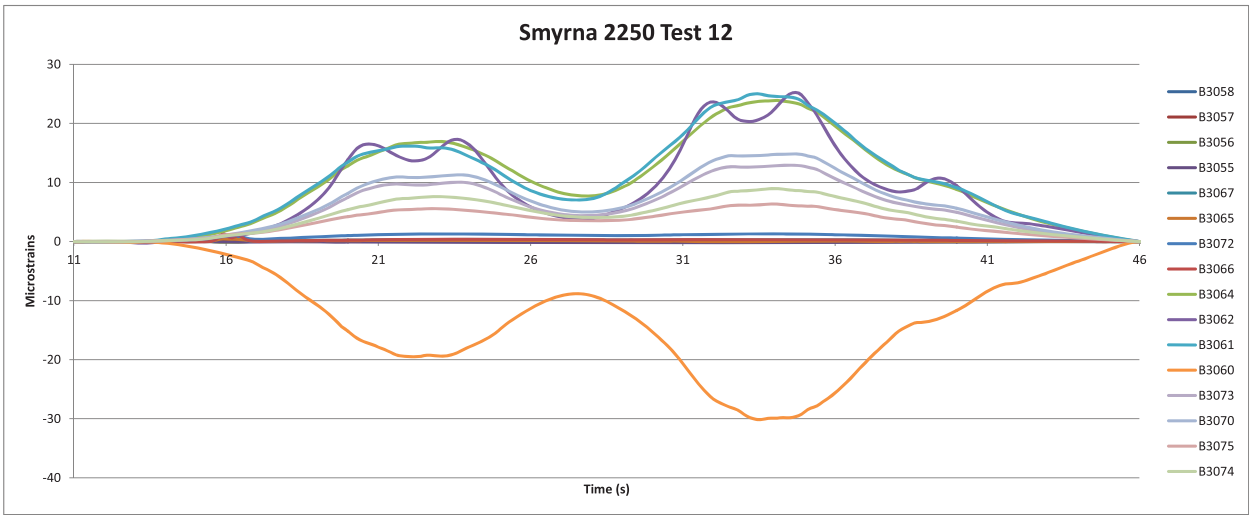

Figure 47: Smyrna No. 2250, test 12

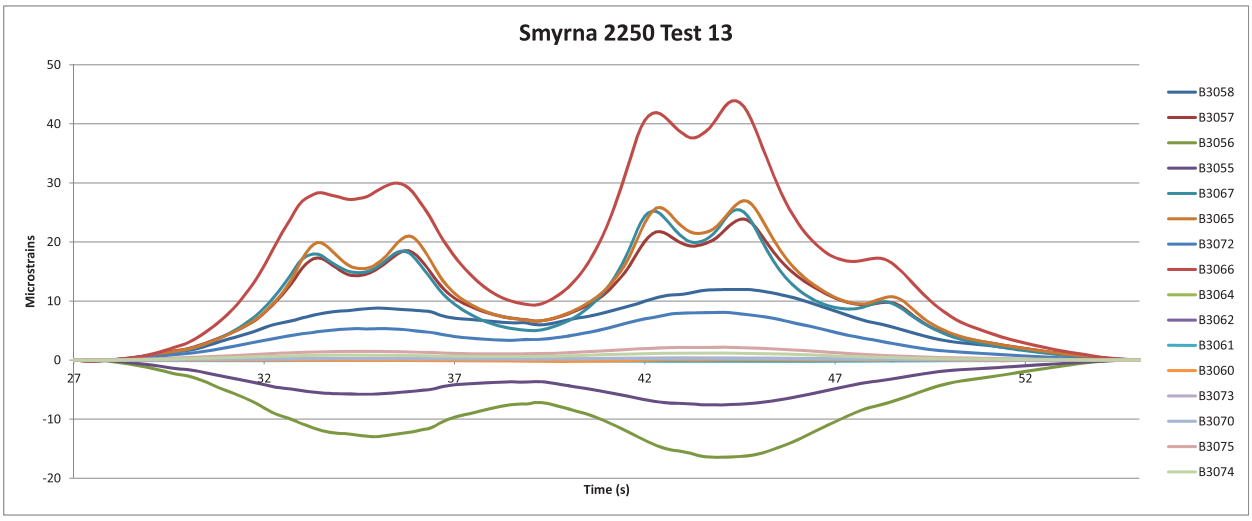

Figure 48: Smyrna No. 2250, test 13

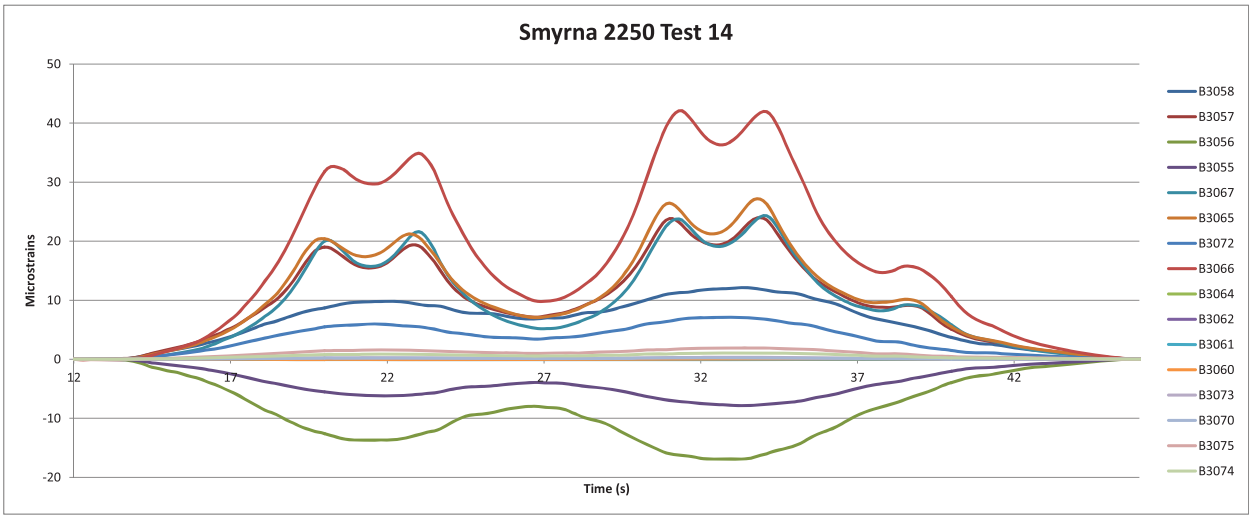

Figure 49: Smyrna No. 2250, test 14